

## Evolution of horn length and lifting strength in the Japanese rhinoceros beetle *Trypoxylus dichotomus*

### Highlights

- Biomechanical costs of extreme structures are often hidden by compensatory traits
- We trace the evolution of long horns in a beetle and measure the effect on strength
- Horns increased in length twice, yielding weapons with weaker lifting forces
- Some populations later grew taller heads or shorter horns, restoring lifting force

### Authors

Jesse N. Weber, Wataru Kojima,  
Romain P. Boisseau, ..., Laura Corley  
Lavine, Brook O. Swanson, Douglas J.  
Emlen

### Correspondence

jnweber2@wisc.edu (J.N.W.),  
doug.emlen@mso.umt.edu (D.J.E.)

### In brief

Weber et al. document a biomechanical tradeoff associated with the evolution of an exaggerated animal weapon. When beetle horns got long, they also got weaker—a cost that was later ameliorated in some populations. Reconstructing the sequence of evolution of this weapon provides a rare glimpse of an ephemeral and elusive cost to extreme structures.

## Article

# Evolution of horn length and lifting strength in the Japanese rhinoceros beetle *Trypoxylus dichotomus*

Jesse N. Weber,<sup>1,13,\*</sup> Wataru Kojima,<sup>2,13</sup> Romain P. Boisseau,<sup>3,13</sup> Teruyuki Niimi,<sup>4</sup> Shinichi Morita,<sup>4</sup> Shuji Shigenobu,<sup>5</sup> Hiroki Gotoh,<sup>6</sup> Kunio Araya,<sup>7</sup> Chung-Ping Lin,<sup>8</sup> Camille Thomas-Bulle,<sup>3,12</sup> Cerisse E. Allen,<sup>3</sup> Wenfei Tong,<sup>9</sup> Laura Corley Lavine,<sup>10</sup> Brook O. Swanson,<sup>11,14</sup> and Douglas J. Emlen<sup>3,14,15,\*</sup>

<sup>1</sup>Department of Integrative Biology, University of Wisconsin-Madison, Madison, WI 53706, USA

<sup>2</sup>Graduate School of Sciences and Technology for Innovation, Yamaguchi University, 1677-1 Yoshida, Yamaguchi 753-8511, Japan

<sup>3</sup>Division of Biological Sciences, The University of Montana, Missoula, MT 59812, USA

<sup>4</sup>Division of Evolutionary Developmental Biology, National Institute for Basic Biology, 38 Nishigonaka Myodaiji, Okazaki 444-8585, Japan

<sup>5</sup>Trans-Scale Biology Center, National Institute for Basic Biology, 38 Nishigonaka Myodaiji, Okazaki 444-8585, Japan

<sup>6</sup>Department of Science, Graduate School of Integrated Science and Technology, Shizuoka University, 836 Oya, Suruga Ward, Shizuoka, Japan

<sup>7</sup>Faculty of Social and Cultural Studies, Kyushu University, 744 Motooka, Nishi-ku, Fukuoka-city Fukuoka 819-0395, Japan

<sup>8</sup>Department of Life Science, National Taiwan Normal University, No.88 Sec. 4, Tingzhou Rd, Taipei 11677, Taiwan

<sup>9</sup>Cornell Laboratory of Ornithology, Ithaca, NY 14850, USA

<sup>10</sup>Department of Entomology, Washington State University, Pullman, WA 99164, USA

<sup>11</sup>Department of Biology, Gonzaga University, 502 East Boone Avenue, Spokane, WA 99258-0102, USA

<sup>12</sup>Department of Biological Sciences, University of Denver, Denver, CO 80208, USA

<sup>13</sup>These authors contributed equally

<sup>14</sup>Senior author

<sup>15</sup>Lead contact

\*Correspondence: [jnweber2@wisc.edu](mailto:jnweber2@wisc.edu) (J.N.W.), [doug.emlen@mso.umt.edu](mailto:doug.emlen@mso.umt.edu) (D.J.E.)

<https://doi.org/10.1016/j.cub.2023.08.066>

## SUMMARY

What limits the size of nature's most extreme structures? For weapons like beetle horns, one possibility is a tradeoff associated with mechanical levers: as the output arm of the lever system—the beetle horn—gets longer, it also gets weaker. This “paradox of the weakening combatant” could offset reproductive advantages of additional increases in weapon size. However, in contemporary populations of most heavily weaponed species, males with the longest weapons also tend to be the strongest, presumably because selection drove the evolution of compensatory changes to these lever systems that ameliorated the force reductions of increased weapon size. Therefore, we test for biomechanical limits by reconstructing the stages of weapon evolution, exploring whether initial increases in weapon length first led to reductions in weapon force generation that were later ameliorated through the evolution of mechanisms of mechanical compensation. We describe phylogeographic relationships among populations of a rhinoceros beetle and show that the “pitch-fork” shaped head horn likely increased in length independently in the northern and southern radiations of beetles. Both increases in horn length were associated with dramatic reductions to horn lifting strength—compelling evidence for the paradox of the weakening combatant—and these initial reductions to horn strength were later ameliorated in some populations through reductions to horn length or through increases in head height (the input arm for the horn lever system). Our results reveal an exciting geographic mosaic of weapon size, weapon force, and mechanical compensation, shedding light on larger questions pertaining to the evolution of extreme structures.

## INTRODUCTION

Competition for access to reproduction (sexual selection) can lead to rapid increases in male weapon size.<sup>1,2</sup> Because these weapons are deployed against the weapons of conspecific rivals, an aspect of the social environment that is itself evolving, male competition can generate consistent and intense directional selection for elaborations to weapon form that improve

contest outcome.<sup>3–6</sup> For many weapons, this means increases in length or overall weapon size.<sup>2,7–11</sup>

Longer weapons permit a male to touch, strike, grab, or flip an opponent before that rival can do the same.<sup>12–16</sup> Longer weapons may also function as agonistic signals—deterrants—settling contests before they escalate into dangerous battles.<sup>12,14,17–29</sup> When opponents are evenly matched, however, even these contests escalate, and this means that weapons

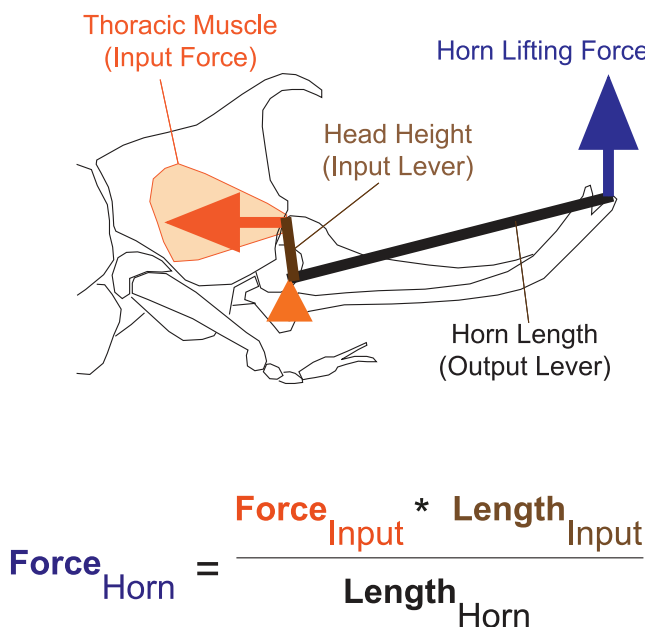


**Figure 1. Force-producing lever mechanics of the rhinoceros beetle head horn**

Horn lever system of *Trypoxylus dichotomus*. Males attempt to insert their horn underneath an opponent and lift them off the sides of trees. Lifting forces (blue arrow) are generated by a lever system, comprising an output lever (horn length), an input lever (head height), and muscles housed in the thorax that rotate the head (input force, orange arrow) to lift the horn. The fulcrum (orange triangle) is located in the head between the input and output levers.

cannot solely serve as signals, they must also function as tools of battle.<sup>30–33</sup>

Although longer weapons may be advantageous for their added reach and as deterrent signals, longer is not necessarily better for generating force.<sup>32,34–36</sup> Weapons that lift, pry, or squeeze function as lever systems and include an “output” lever (e.g., a horn), an “input” lever (e.g., a rigid head), and muscles attached to the input lever that, when contracted, rotate both levers about a fulcrum (Figure 1).<sup>37</sup>

The force generated by the weapon can be predicted from the relative lengths of the two levers and the size of the associated muscles:

$$\text{Force}_{\text{output lever}} = (\text{Force}_{\text{input lever}} * \text{Length}_{\text{input lever}}) / \text{Length}_{\text{output lever}} \quad (\text{Equation 1})$$

For most animal weapons, the output levers (i.e., horns, tusks, antlers) are not physically constrained from expanding, protruding as they do from the body. The input levers and associated musculature, in contrast, are housed inside the body where limitations of space may constrain their size.<sup>35</sup> Strong sexual selection driving rapid increases in weapon length can create an imbalance with the rest of the lever system, yielding tools that lift, pry, or squeeze with reduced force.<sup>32,35,38–40</sup>

In principle, this “paradox of the weakening combatant”<sup>34</sup> could limit the elaboration of sexually selected weapons if increases in weapon length reduced force enough to offset signaling or other benefits. However, studies of the biomechanical force generation

of animal weapons generally find that forces are maintained, even in the longest-weaponed individuals, due to the presence of compensatory changes to the lever system. In crabs, frog-legged beetles, stag beetles, and leaf-footed bugs, increases in relative muscle size maintain weapon performance as weapon lengths increase,<sup>35,38,41,42</sup> and in stag beetles and frog-legged beetles the relative length of input levers increases as well.<sup>38</sup>

To date, most biomechanical studies focus on individual variation within populations (e.g., static allometry of input and output levers and relative muscle size), clearly demonstrating a variety of means to mechanical compensation.<sup>32,34,35,38,39,43–47</sup> A few studies extend to multiple populations or species,<sup>39,40,48–51</sup> but none so far include sufficient information about the historical relationships of populations to permit a full reconstruction of the dynamic stages of weapon evolution and the accompanying origin and spread of mechanical compensation.

Here, we present results from a comprehensive phylogeographic study of a large-weaponed species, the Asian rhinoceros beetle *Trypoxylus dichotomus*<sup>52</sup> (Coleoptera, Scarabaeidae). We collected samples from 23 locations across the range of this species and used high-throughput DNA sequencing approaches to consolidate these into nine genetically and morphologically distinguishable populations. Using the closest sister species (*Xyloscaptus davidis*) as an outgroup, we reconstruct the historical relatedness among these populations and use this tree to examine the evolution of both weapon size and weapon lifting strength.

We show that the most parsimonious model of horn evolution involves initial increases in weapon size associated with significant reductions to lifting strength, but this mechanical disadvantage was later ameliorated, to some extent and in some locations, either by subsequent reductions to horn length or by an increase in input lever length (head height). In addition, some populations differ in the amount of muscle powering the horn lifting system, suggesting another mode of compensation. Our results reveal an exciting geographic mosaic of differences in weapon size, weapon force, and in the extent and nature of mechanical compensation, highlighting the utility of leveraging extant variation among populations and their historical relatedness to characterize biomechanical tradeoffs associated with extreme weapon evolution.

*T. dichotomus* is a univoltine scarab whose larvae feed in the soil on decaying wood, emerging as adults in early June to mid-July, depending on the location.<sup>53–58</sup> Adult behavior has been studied most extensively on Honshu Island, Japan, where beetles fly to wounds on the sides of mature oak, ash, and maple trees (e.g., *Quercus mongolica*, *Q. acutissima*, *Q. serrata*, *Fraxinus griffithii*, *Acer plantanoides*)<sup>55</sup> and feed on oozing sap.<sup>13,55,58,59</sup> Females fly to these territories to feed and mate, before leaving to lay eggs in decomposing litter up to a kilometer or more away.<sup>60,61</sup>

Males battle with rival males for ownership of feeding territories, and the largest males with the longest horns are most likely to win.<sup>13,55,57,58,62,63</sup> Territorial males turn to face rival males as they approach, sweeping their horn until it touches the opponent. Both males then push with their horns in brief, shoving lunges that usually result in the smaller male aborting the confrontation and being chased away by the larger male.<sup>13</sup> Sensory hairs on the surface of the horns are densest in regions

that touch during contests,<sup>64</sup> and horns appear to function as tactile signals of resource-holding potential during these early “shoving” stages of battles.<sup>13</sup>

When these pushes fail to resolve the contest, then fights escalate. Males insert the tip of their horn beneath the body of the other male and attempt to pry him off the tree. The pitch-fork-shaped head horn functions as a simple lifting lever, with the junction of the head and thorax serving as a fulcrum (Figure 1). The head acts as the input lever and is attached to large muscles housed in the thorax, which rotate the head to raise the horn.<sup>50</sup> Males strain visibly during these ritualized contests of strength,<sup>47</sup> and fights end when one of the males gives up and runs away, or when a male loses his footing and is flung to the ground.<sup>13,57</sup> Both lifting/tying and clinging (resisting) forces have been measured in the field,<sup>47,50,65</sup> and exerted forces are large enough that escalated contests sometimes lead to mechanical failure of the horn. In one study, 17% of the males showed visible injuries consistent with this escalated “tying” stage of fighting and 4% of males had broken and lost their horn.<sup>47</sup>

Horns in *T. dichotomus* thus appear to function as both agonistic deterrent signals and as mechanical tools, and males in at least some populations experience strong directional selection for increases in horn length (e.g., Kyoto, Japan<sup>13,55</sup>; Kameoka, Japan<sup>57</sup>), suggesting this weapon may have been susceptible to the paradox of the weakening combatant. Rapid evolutionary increases in output lever (horn) length could have outpaced the rest of this lever system, resulting in a reduction to the lifting force generated by the horns. If true, then *T. dichotomus* horns may have experienced selection for mechanisms that ameliorate the mechanical disadvantage of long horns.<sup>34</sup> Preliminary studies demonstrate that within populations, large males compensate for their long horns with relatively larger thoracic lifting muscles than smaller males.<sup>50</sup> But populations of this species are known to differ in horn length<sup>57,66</sup> and in horn lifting strength,<sup>50</sup> motivating the present study. We reconstruct the historical and phylogeographic relationships among *T. dichotomus* populations and use these relationships to test whether initial increases in male horn length resulted in reductions to horn lifting force that were later ameliorated through the evolution of compensatory traits.

## RESULTS

### Genetic structure of *T. dichotomus* populations

After filtering, our population structure dataset contained 198 individuals genotyped across 13,547 loci. See **STAR Methods** and **key resources table** for subspecies and sample locations. Admixture analyses suggest that the genetic variation in *T. dichotomus* is best explained (CV error = 0.22752) by grouping individuals into the following six general subpopulations: Japan central; Japan south, including Goto island; Kuchinoerabu-Yakushima-Tanegashima islands; Okinawa-Kumejima islands; Taiwan; and mainland China (Figure 2).  $k = 5$  populations also provided a good fit (CV error = 0.22828), with the main difference being that the small islands of Kuchinoerabu, Yakushima, and Tanegashima, which lie off the southern coast of the larger island of Fukuoka, Japan, cluster with one of the Japanese main island populations.

Beetles from *T. kanamorii* and *T. d. politus* each showed a mixture of genetic backgrounds; however, it is unclear whether this pattern results from vicariance followed by incomplete lineage sorting or from recent gene flow between divergent lineages. Because these subspecies are clearly distinguishable morphologically, and both are rare and confined to the far western part of the range (Myanmar and Thailand, respectively), we treated them as separate populations in this study. Beetles on Goto island cluster with the southern Japanese main island population and were not distinguishable in our admixture analysis. However, males on Goto island are morphologically distinct from mainland beetles (relatively shorter horn lengths; Figure 3), so we treated Goto as a separate population for horn length and horn strength analyses. Consequently, we assigned beetles into nine genetically and/or morphologically recognizable populations (Figure 2) and used these groupings of individuals for the subsequent horn length and horn strength analyses.

### Historical phylogeography of *T. dichotomus*

Both the combined analysis with *X. davidis* as an outgroup and the separate northern and southern clade analyses, each with a representative of the other clade as outgroup, yielded the same tree topology, and all but one node had posterior probabilities of 1.0 (Figure 2). Our results clearly support a deep early split between northern and southern populations of beetles, and this split appears to pre-date the branching of *T. kanamorii* and *T. d. politus*.

The northern lineage includes two clusters on the Japanese main islands (*Trypoxylus dichotomus septentrionalis*) and a cluster that includes three of the tiny offshore islands, Kuchinoerabu (*T. d. tsuchiyai*) and Yakushima and Tanegashima (*T. d. shizuae*) (Figure 2). The southern lineage includes *T. kanamorii* and *T. d. politus* (sampled from Myanmar and Thailand, respectively), as well as Okinawa-Kumejima (*T. d. takarai/T. d. inchachina*), mainland China (*T. d. dichotomus*), and Taiwan (*T. d. tsunobosonus*).

*T. kanamorii* and *T. d. politus* were predicted to be the most basal lineages in our study, based both on geographic location and on morphological taxonomy,<sup>67,68</sup> and our population genetic results suggest they each contain mixtures of alleles from both northern and southern populations. However, our coalescent analyses strongly support placement of these populations within the southern lineage rather than at the base of the combined *T. dichotomus* tree. If true, then this would indicate that long horns likely evolved independently in the northern and southern lineages (see below).

The islands Okinawa and Kumejima also share alleles with both northern and southern populations, yet they too clearly branch from the southern lineage. In the case of *T. kanamorii* and *T. d. politus*, we suspect that the shared alleles may reflect genetic variation present in an ancestral population predating the north-south split. This may also be true for Okinawa-Kumejima. However, their location roughly equidistant between Japan and Taiwan suggests that secondary colonization and gene flow could also account for the mixture of north-south alleles that they contain. Additional studies will be needed to resolve these issues more fully. Regardless, our results provide a well-supported tree sufficient for reconstructing historical patterns of evolution of horn length and horn strength.

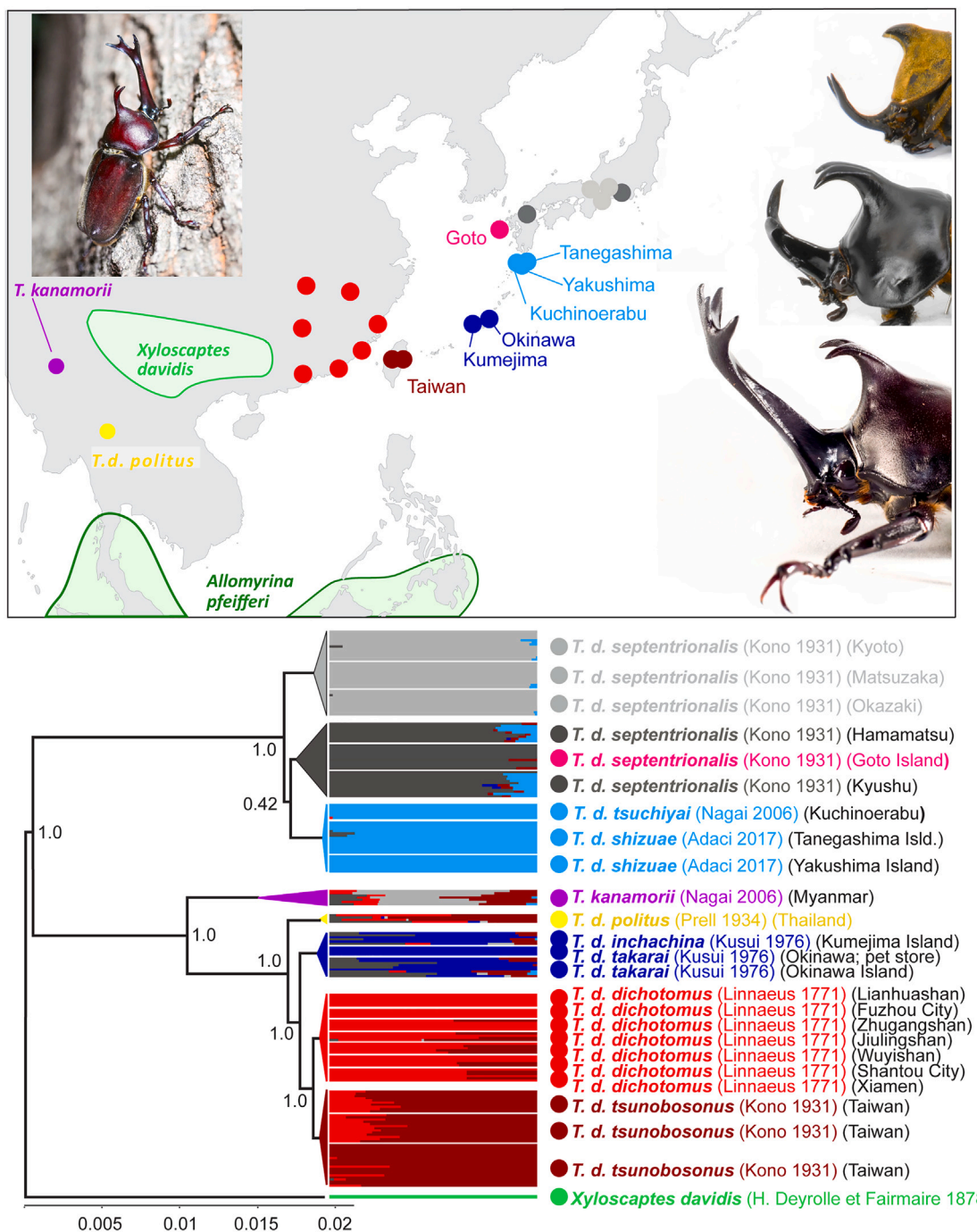


**Figure 2. Sample locations, genetic structure, and phylogeny of the populations examined**

Top: sample locations and head horns of *Trypoxylus dichotomus* (insert, bottom), its closest sister species *Xyloscaptus davidis* (middle), and the next most closely related species, *Allomyrina pfeifferi* (top), for comparison. Bottom: ancestral relationships among populations of *T. dichotomus*. Genetic structure analyses show that individuals cluster into 6 primary populations: Japan central (light gray), Japan south (dark gray), Kuchinoerabu/Yakushima/Tanegashima islands (light blue), Okinawa/Kumejima (dark blue), mainland China (red), and Taiwan (maroon). *T. kanamorii* (purple) and *T. d. politus* (yellow) were also considered to be separate populations, based on morphology and geographic location. Goto island beetles, although placed within the Japan south cluster, were also morphologically distinct and thus were treated as a separate population for horn length and horn strength comparisons. Clade support values represent Bayesian posterior probabilities. Branch lengths represent substitutions per site.

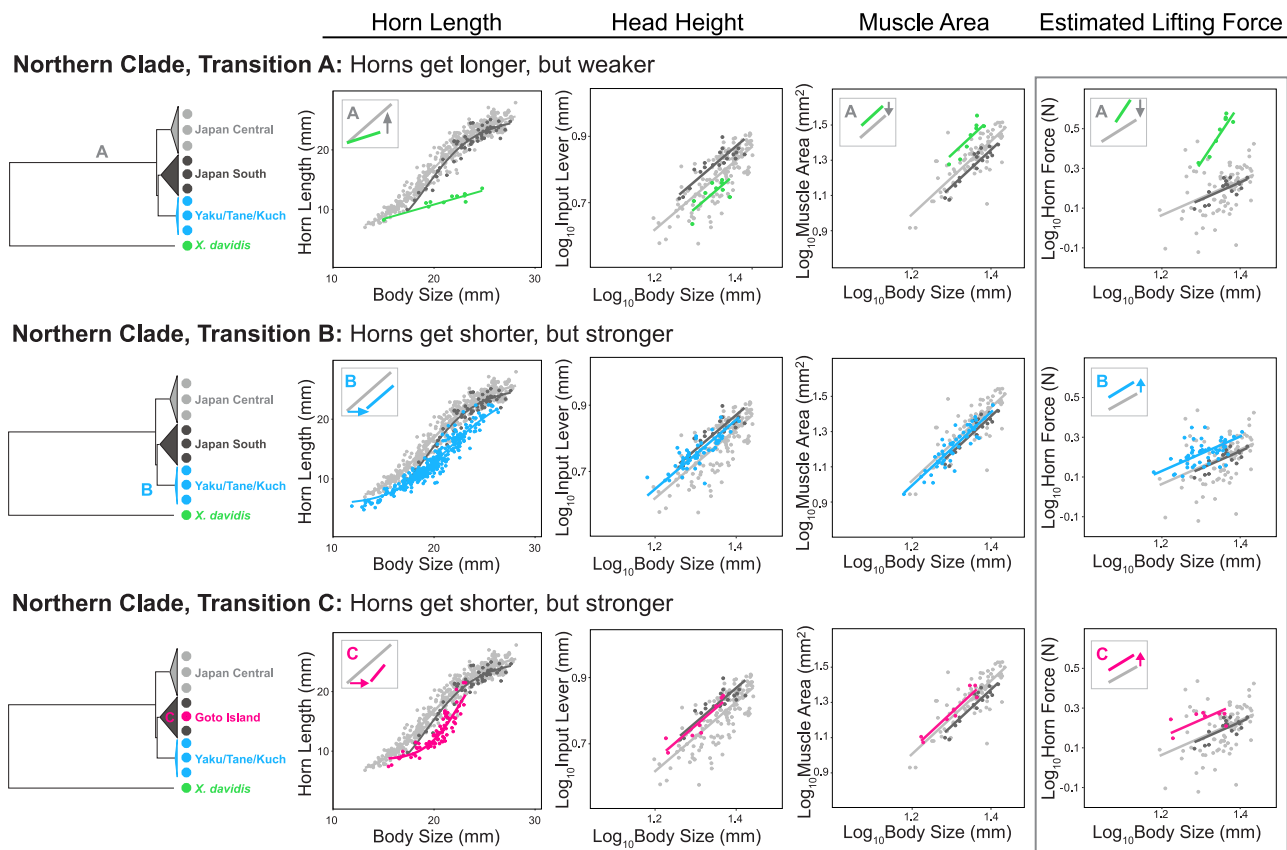


**Figure 3. Male horns get long and weak, then shorter and stronger in the northern clade of rhinoceros beetles**

Inferred transitions in horn length, head height (input lever length), muscle area, and estimated horn lifting force in the northern lineage of *T. dichotomus*. Horns of *X. davidis* (green) were considered to represent the ancestral morphology of this species. Significant population differences are indicated by insets. Analyses are presented in Tables S1–S6. See also Figures S1 and S2.

#### Evolution of male horn length

*T. dichotomus* males had relatively longer horns and their horn length/body size allometry had a steeper slope than males of the most closely related sister species, *X. davidis* (Figures 3, 4, and S1; Table S1).

When *Trypoxylus* populations were mapped onto the phylogeographic tree and compared using parameter substitutions to a sigmoid curve (Figures S1C and S1D; Tables S2 and S3), horn evolution was reconstructed as follows. In the north (Figure 3), *Trypoxylus* experienced a dramatic early increase in relative horn length resulting from an increase in the slope of the horn length/body size scaling relationship (transition A), leading to long-horned beetles in the Japanese main islands. Then, presumably as beetles colonized the tiny offshore islands of Kuchinoerabu, Yakushima, and Tanegashima, horn sizes got smaller as the allometry intercept shifted to a larger body size (transition B). Finally, although our admixture analyses still cluster Goto island beetles with the Japan south population, the horn lengths of Goto males are significantly shorter than main island beetles, resulting from a shift in the allometry intercept and an increase in allometry steepness (transition C). Interestingly, although the relative horn lengths (intercepts) of Goto and Kuchinoerabu-Yakushima-Tanegashima beetles do not differ—males have

relatively short horns in all of these islands—the steepness of the sigmoid scaling relationship does differ between Goto and the other offshore island populations (Figure 3; Table S2), a morphological difference consistent with our genetic evidence, which suggests a separate colonization event and an independent evolutionary reduction in relative horn length.

In the southern clade (Figure 4), male horns also increased in length. Both *T. kanamorii* and *T. d. politus* are rare, and we were only able to measure three male specimens of *T. kanamorii* for this study. However, both subspecies are known to have very short horns, and the three male *T. kanamorii* we included fell along the same horn length/body size allometry as the short-horned sister species *X. davidis* (Figure S1A). From these short-horned ancestors, beetles appear to have evolved several changes in horn length. Understanding the directions and magnitude of change in horn length in this southern lineage depends on knowing the state of the last common ancestor of Okinawa-Kumejima and mainland China animals, which is difficult to interpret given that there are too few lineages to perform a robust ancestral state calculation and recent studies show that island ecologies favor shorter horns.<sup>57,69,70</sup> At least one change in horn length occurred in Okinawa-Kumejima males. For simplicity, we describe this as an evolutionary increase leading

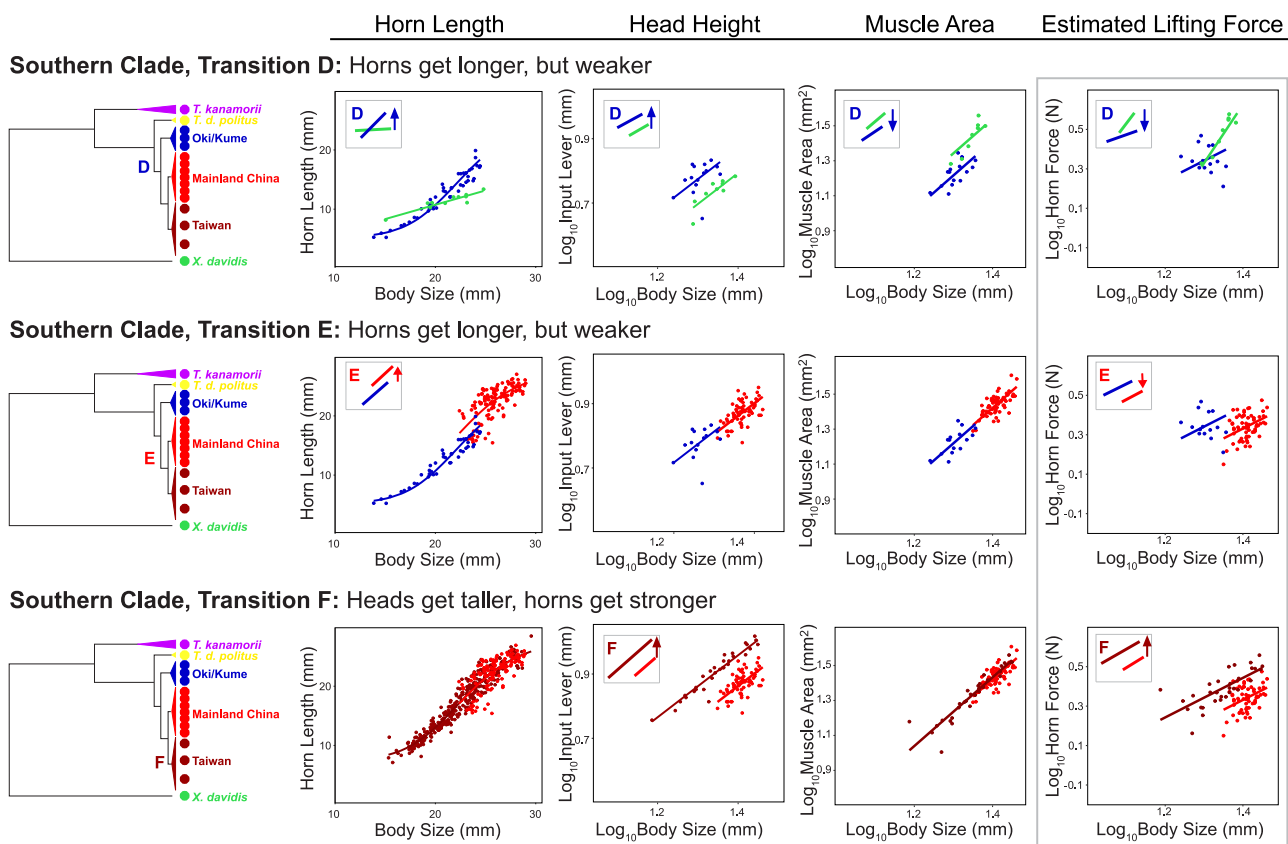


**Figure 4. Male horns get long and weak, then stay long but get stronger in the southern clade of rhinoceros beetles**

Inferred transitions in horn length, head height (input lever length), muscle area, and estimated horn lifting force in the southern lineage of *T. dichotomus*. Horns of *X. davidis* (green) were considered to represent the ancestral morphology of this species. Significant population differences are indicated by insets. Analyses are presented in Tables S1–S6. See also Figures S1 and S2.

to a slightly steeper allometry than *X. davidis* (transition D). A second evolutionary change involved an increase in both allometry steepness and intercept in the lineage of long-horned males of the mainland China and Taiwan populations (transition E).

#### Evolution of the horn lever system: Head height, thoracic muscle area, and estimates of horn lifting force

Population comparisons of head height (input lever length), relative muscle size, and horn lifting force are presented in Figure S2 and Tables S4–S6.

In the north, the initial increase in relative male horn length (output lever length) resulted in a significant reduction in horn lifting force (transition A in Figure 3 and Table S4). However, when beetles colonized the offshore islands Kuchinoerabu-Yakushima-Tanegashima and Goto, male horn lengths subsequently evolved to shorter lengths, leading to increases in horn lifting strength (transitions B and C in Figure 3 and Table S5).

In the south, males in Okinawa-Kumejima evolved changes in both horn length (transition D) and head height (input lever length), so that they lift with the same relative horn strength as *X. davidis* (Figure 4). However, as horn length increased in the lineage leading to the long-horned males of the mainland China population (transition E), head height did not change and these beetles wield weapons with significantly weaker forces than their

shorter-horned ancestors (Table S6). Interestingly, males in Taiwan have the same muscle mass and horn lengths relative to body size as mainland China males but, due to a dramatic evolutionary increase in head height, they lift with significantly stronger forces than their mainland counterparts (transition F) (Table S6).

#### DISCUSSION

Our phylogenetic and population structure results (Figure 2) agree overall with a recent study using specific-locus amplified fragment sequencing.<sup>71</sup> For example, Yang et al.<sup>71</sup> also find a deep split between northern and southern populations; they also place *T. kanamorii* and *T. d. politus* within the southern clade, rather than basal to the *Trypoxylus* tree; and they also find Okinawa-Kumejima beetles to be genetically very distant from other populations (see also Nakada et al.<sup>72</sup>). However, Yang et al.<sup>71</sup> place Okinawa-Kumejima in a cluster with Taiwan beetles, whereas we find Taiwan strongly and closely related to beetles from mainland China.

The Ryukyu archipelago formed sometime between the Cretaceous and early Miocene (>12 million years ago [mya]) along the eastern rim of a contiguous terrestrial continental shelf,<sup>72,73</sup> and many plants,<sup>74,75</sup> mammals,<sup>76</sup> termites,<sup>77</sup> and stag beetles<sup>78</sup>

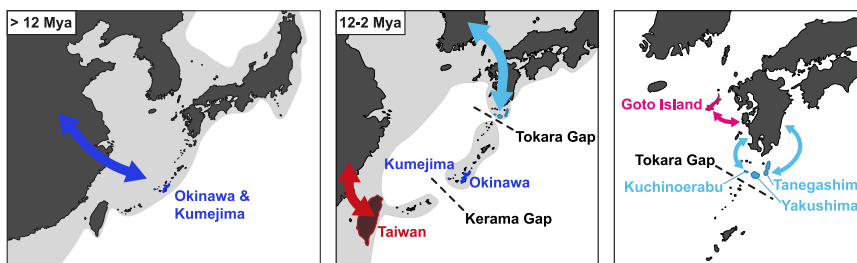


**Figure 5. Proposed biogeographic history of beetles in the Ryukyu archipelago**

Hypothesis for the colonization history and ancestral relationships among populations of *T. dichotomus*.

colonized the region at this time, before rising sea levels isolated islands in the chain. A recent fossil-calibrated molecular clock study estimated the divergence time for the split between *X. davidis* and *T. dichotomus* at 29 mya (95%: 18–44 mya),<sup>79</sup> so ancestral populations of *Trypoxylus* likely would have been present when the Ryukyu islands were still connected to the mainland continental shelf. We suspect that *T. dichotomus* first colonized the islands at this time (Figure 5A) and were subsequently stranded when sea levels rose and cut off the Ryukyu island chain.

Repeated drops in sea level during Pleistocene glaciation cycles temporarily re-connected islands at the northern and southern ends of the Ryukyu chain to the mainland (Figure 5B), providing episodic opportunities for mainland beetles to re-colonize some of the islands, hybridizing with or replacing existing populations. In contrast, beetles living in the middle of the archipelago (e.g., Okinawa, Kumejima) may have remained stranded due to deep oceanic trenches separating them from islands to the north and south (Tokara and Kerama gaps, respectively<sup>72</sup>). This would account for both the ancestral horn morphology of these beetles (see below) and their genetic distance from beetles on islands to the north and south.<sup>80</sup> The climatic and faunal records are also more consistent with our phylogenetic result, placing the Okinawa-Kumejima cluster distinct from the one containing Taiwan and China, the latter of which would have had multiple opportunities to exchange migrants when the lands were connected during Pleistocene ice ages.

Our genetic data also suggest that colonization of the tiny islands adjacent to the Japanese main islands (Goto, Kuchinoerabu, Yakushima, Tanegashima) occurred at least twice and much more recently than colonization of Okinawa-Kumejima, either across the Pleistocene land bridges (Figure 5B) or through dispersal events from the main islands (Figure 5C). Subsequent studies of gene flow and demography will be needed to better test these hypotheses.

Horns in *T. dichotomus* almost certainly started small. Both of the sister species, *X. davidis* and *Allomyrina pfeifferi*, and the two most basal populations of *Trypoxylus*, *T. kanamorii*, and *T. d. politus*, have short horns, and beetles isolated on the mid-Ryukyu islands of Okinawa and Kumejima have horns only slightly longer. Then, based on our genetic and phylogeographic results, male horn lengths increased dramatically 2 times, more than doubling in length along both the northern and southern lineages, respectively.

Both increases in horn length resulted from the evolution of steeper horn length/body size allometry slopes (Figures 3 and 4; Table S1). For decades, biologists have debated the extent to which morphological trait allometries constrain the evolution

of animal morphology,<sup>81–87</sup> and the slope in particular is famously conserved.<sup>86–88</sup> Numerous artificial selection experiments have altered the slope of a static trait allometry (e.g., wing size in *Drosophila melanogaster*<sup>89,90</sup> and the butterfly *Bicyclus anynana*<sup>91</sup> and eyestalk length in the fly *Cyrtodiopsis dalmanni*<sup>92</sup>), and developmental genetic studies now point toward candidate genes and physiological pathways that could contribute to static allometry slope evolution.<sup>93–102</sup> Yet it is also clear that changing a static allometry slope is not easy—responses to selection are erratic and much slower than responses to selection applied to the intercept of these same allometries.<sup>89,90</sup> Indeed, a meta-analysis of more than 300 empirical studies of static trait allometry evolution concluded that allometry slopes likely change slowly over long timescales (>1 million years) in contrast with allometry intercepts, which routinely differ among local populations.<sup>86</sup> It is noteworthy in this respect that our results point to evolutionary increases in allometry slope occurring in the deepest branches of our analysis, as the northern and southern lineages of *Trypoxylus* diverged from their shared common ancestor with *X. davidis*—a split estimated to have occurred almost 30 mya<sup>79</sup>—while all of the evolutionary changes to horn allometry that we observe among local populations of *Trypoxylus* involve shifts in allometry intercept rather than slope (Figures 3 and 4).

In the context of animal communication, increases in static allometry slope are predicted for strongly sexually selected structures,<sup>103–108</sup> particularly those that function as signals in agonistic assessment or mate choice.<sup>109–113</sup> Specifically, a steeper static allometry slope increases the range of among-male variation in trait size (hypervariability), amplifying otherwise-subtle differences in underlying male condition so that they are easier for receivers to perceive.<sup>114–119</sup>

The evolution of steep static allometry often results from increases in the developmental plasticity or nutrition-sensitivity of trait growth,<sup>94–96,100,120</sup> and this “heightened,” condition-sensitive expression is yet another characteristic common to conspicuous structures that function as reliable signals of male body size or condition.<sup>96,120–124</sup> Indeed, such heightened conditional expression has already been demonstrated for the horns of this species.<sup>96,125</sup> Consequently, the dramatic increases in static allometry slope observed in the northern and southern lineages of *T. dichotomus* are consistent with animals beginning to use this structure as a deterrent signal during contests.

Male-male interactions also suggest that horns function as tactile signals of resource-holding potential (*sensu* Searcy and Beecher<sup>126</sup>). The poking and shoving that males do<sup>13</sup> aligns with dense patches of sensory hairs on the surface of the horns,<sup>64</sup> and most confrontations are settled at this initial shoving

stage of the contest.<sup>13,57,63</sup> In this respect, male horns are similar to other enlarged, cuticular weapons in insects that also function as tactile signals in male contests (e.g., weevils,<sup>27,127</sup> leaf-footed bugs,<sup>128,129</sup> tree wetas,<sup>24</sup> frog-legged leaf beetles,<sup>130</sup> flower beetles,<sup>15</sup> and stag beetles<sup>28</sup>).

However, as in these other species, evenly matched *T. dichotomus* males escalate contests beyond the initial stages of assessment, and when this happens, the weapons must also function as biomechanical levers. Males in all populations studied to date position their head horn underneath the body of an opponent, straining to lift/pry that rival away from the tree, and males with the largest body sizes and the longest horns consistently win these contests.<sup>13,47,50,55,57–59</sup> Although the relationship between prying strength and mating success has yet to be examined in the field, the details of male behavior suggest that powerful prying forces are integral to male success during the escalated stages of matched battles and therefore critically relevant to a male's ability to defend a feeding (and mating) territory. The unusual, triangular cross-sectional shape of this horn is also consistent with a history of selection for strong prying forces because it specifically resists buckling when the horn is lifted—even when horns are twisted during lifting, as occurs often given the “pitchfork” widening at the tip of this horn.<sup>65,131</sup> Consequently, any evolutionary increases in horn length that weakened male horn lifting strength (the paradox of the weakening combatant)<sup>34</sup> could have negatively impacted male fight success in ways that offset the signaling advantages of an ever longer horn, potentially leading to the evolution of compensatory traits that restored strength to these weapons.

We show that the two most dramatic increases in male horn length in this species were each accompanied by significant reductions to horn lifting strength (transitions A and E in Figures 3 and 4, respectively), consistent with the paradox of the weakening combatant.<sup>34</sup> Then, as beetles colonized the northern Ryukyu islands of Kuchinoerabu-Yakushima-Tanegashima and Goto, male horns subsequently evolved to be relatively shorter, restoring (increasing) their lifting strength in each instance. This may be the result of selection for horn strength offsetting the benefits of long horns, shifting the balance of selection on this structure. Alternatively, local changes to the breeding ecology of the beetles may have relaxed the strength of selection on horn length. Field observations of contemporary populations on Yakushima island suggest that beetle densities are much lower than on the mainland and that feeding territories are more numerous, both of which could detract from the fitness benefits of long horns<sup>57,66</sup> (W.K., personal observation). On Goto island, beetle densities are sometimes high and male fights and fight-related injuries are prevalent (W.K., personal observation), so the recent reduction in horn length could be interpreted as compensatory evolution to restore horn lifting strength.

In the southern lineage of *Trypoxylus*, we see compelling evidence for compensatory evolution. When beetles colonized Taiwan, they retained the long horn lengths of their mainland Chinese neighbors, but these animals have ameliorated the associated reduction in horn lifting strength through an evolutionary increase in the height of their heads. Taller heads increase the length of the input lever (Figure 1), compensating for the long head horn and restoring strength to this exaggerated male weapon (Figure 4). Evolutionary elongation of stag beetle

(Lucanidae) mandibles also appears to have been accompanied by compensatory increases in the length of the input lever.<sup>39</sup> The lever system of the stag beetle mandible rotates from side-to-side, in contrast with the up-down lifting rotation of *T. dichotomus* horns, so increases in stag beetle input lever length resulted in wider, rather than taller, male heads, as well as substantially stronger mandible-squeezing forces.<sup>39</sup>

Field studies of contemporary populations on Taiwan consistently observe high densities of beetles—the highest yet recorded for this species—and male battles are both intense and frequent (dozens per territorial male per night<sup>47,57,60,61</sup>), as would be expected if selection for male fight performance were driving the evolution of mechanical compensation at this location. However, the increase in input lever length of the Taiwanese beetles should also decrease the amount of muscle needed to produce a given force. Therefore, the increased mechanical advantage seen in Taiwanese beetles could be an example of selection for increased force, or for decreased energetic cost for producing a given force, both of which may be advantageous in a population with extensive and frequent battles.

Here, we assume that horn force production is important for winning fights, and observations of both fighting behavior<sup>13,57</sup> and beetle grip strength<sup>47</sup> suggest that this is likely true. However, there are alternative biomechanical interpretations of the variation in morphology that we see across populations. The function of the horn during male battles is complicated, especially during the early shoving stages when males appear to use their horns to assess each other.<sup>13</sup> Horns poke, strike, or push opponents from several different orientations, and it is possible that length (i.e., being able to touch a rival before that beetle can touch you) is more important than lifting strength in these early stages of the interaction. Speed may be important too, and this also could select for longer horn lengths because there should be a force versus speed tradeoff associated with horn length, and a longer horn relative to body size moves faster.<sup>34,37</sup> Additional field studies are underway, which should help elucidate the various functions and forces associated with horn use in this species.

Costs and mechanical tradeoffs are notoriously difficult to measure, even for the exaggerated ornaments and weapons of sexual selection.<sup>132–136</sup> One reason may be the coevolution of compensatory traits, which ameliorate past costs, making them difficult to detect in contemporary populations (reviewed in Oufiero and Garland<sup>137</sup> and Swallow and Husak<sup>138</sup>). Here, we show how population genomics approaches can be used to reconstruct the stages of evolution of a sexually selected male weapon and its associated suite of compensatory traits, revealing strong initial tradeoffs as well as subsequent force-compensation, shedding new light on an old question: what limits the sizes of extreme structures?

## STAR★METHODS

Detailed methods are provided in the online version of this paper and include the following:

- KEY RESOURCES TABLE
- RESOURCE AVAILABILITY
  - Lead contact

- Materials availability
- Data and code availability
- **EXPERIMENTAL MODEL AND SUBJECT DETAILS**
- **METHOD DETAILS**
  - DNA extraction and ddRAD library preparation
  - Mapping and genotyping
- **QUANTIFICATION AND STATISTICAL ANALYSIS**
  - Population genetic analyses
  - Coalescent Analyses and Phylogeny Construction
  - Weapon Size Comparisons
  - Evolution of the horn lever system: head height, thoracic muscle area, and estimates of horn lifting force

#### SUPPLEMENTAL INFORMATION

Supplemental information can be found online at <https://doi.org/10.1016/j.cub.2023.08.066>.

#### ACKNOWLEDGMENTS

This project was funded by the NSF IOS-1456133 (D.J.E.), JSPS 17H06901 (W.K.), The Gonzaga Science Research Program (B.O.S.), NSF IOS-1456731 (L.C.L.), and MOST 103-2311-B-029-001-MY3 and 104-2621-B-003-002-MY3 (C.-P.L.). Benjamin Buchalski and Dylan Scanes helped collect biomechanical measurements. This manuscript benefitted significantly from the constructive comments of three reviewers.

#### AUTHOR CONTRIBUTIONS

D.J.E., B.O.S., C.E.A., and L.C.L. conceived of the study. W.K., J.N.W., W.T., H.G., K.A., and C.-P.L. conducted fieldwork and provided samples. J.N.W. performed ddRAD-seq and admixture analyses. S.S., S.M., and T.N. performed genome sequencing and assembly. W.K. and B.O.S. performed horn and biomechanical measures. R.P.B. and J.N.W. performed the statistical analyses. D.J.E., J.N.W., C.T.-B., and B.O.S. wrote the manuscript.

#### DECLARATION OF INTERESTS

The authors declare no competing interests.

#### INCLUSION AND DIVERSITY

We support inclusive, diverse, and equitable conduct of research.

Received: March 13, 2023

Revised: June 28, 2023

Accepted: August 23, 2023

Published: September 20, 2023

#### REFERENCES

1. Darwin, C. (1871). *The Descent of Man, and Selection in Relation to Sex*2 (Cambridge University Press).
2. Andersson, M. (1994). *Sexual Selection* (Princeton University Press).
3. West-Eberhard, M.J. (1979). Sexual selection, social competition, and evolution. *Proc. Am. Philos. Soc.* 123, 222–234.
4. West-Eberhard, M.J. (1983). Sexual selection, social competition, and speciation. *Q. Rev. Biol.* 58, 155–183.
5. Lyon, B.E., and Montgomerie, R. (2012). Sexual selection is a form of social selection. *Philos. Trans. R. Soc. Lond. B Biol. Sci.* 367, 2266–2273.
6. De Lisle, S.P., Bolnick, D.I., Brodie, E.D., III, Moore, A.J., and McGlothlin, J.W. (2022). Interacting phenotypes and the coevolutionary process: interspecific indirect genetic effects alter coevolutionary dynamics. *Evolution* 76, 429–444.
7. Clutton-Brock, T.H., Albon, S.D., and Harvey, P.H. (1980). Antlers, body size and breeding group size in the Cervidae. *Nature* 285, 565–567.
8. Bro-Jørgensen, J. (2007). The intensity of sexual selection predicts weapon size in male bovids. *Evolution* 61, 1316–1326.
9. Emlen, D.J. (2008). The evolution of animal weapons. *Annu. Rev. Ecol. Evol. Syst.* 39, 387–413.
10. Emlen, D.J. (2014). *Animal Weapons: The Evolution of Battle* (Henry Holt/ Macmillan).
11. Plard, F., Bonenfant, C., and Gaillard, J.M. (2011). Revisiting the allometry of antlers among deer species: male–male sexual competition as a driver. *Oikos* 120, 601–606.
12. Hyatt, G.W., and Salmon, M. (1978). Combat in the fiddler crabs *Uca pugilator* and *U. pugnax*: a quantitative analysis. *Behaviour* 65, 182–211.
13. Hongo, Y. (2003). Appraising behaviour during male–male interaction in the Japanese horned beetle *Trypoxylus dichotomus septentrionalis* (Kono). *Behaviour* 140, 501–517.
14. Goyens, J., Dirckx, J., and Aerts, P. (2015). Stag beetle battle behavior and its associated anatomical adaptations. *J. Insect Behav.* 28, 227–244.
15. Kojima, W., and Lin, C.P. (2017). It takes two to tango: functional roles, sexual selection and allometry of multiple male weapons in the flower beetle *Dicronocephalus wallichii bourgoini*. *Biol. J. Linn. Soc.* 121, 514–529.
16. Fea, M., and Holwell, G. (2018). Combat in a cave-dwelling wētā (Orthoptera: Rhaphidophoridae) with exaggerated weaponry (Orthoptera: Rhaphidophoridae) with exaggerated weaponry. *Anim. Behav.* 138, 85–92.
17. Clutton-Brock, T.H., Albon, S.D., Gibson, R.M., and Guinness, F.E. (1979). The logical stag: adaptive aspects of fighting in red deer (*Cervus elaphus* L.). *Anim. Behav.* 27, 211–225.
18. Enquist, M., and Leimar, O. (1983). Evolution of fighting behaviour: decision rules and assessment of relative strength. *J. Theor. Biol.* 102, 387–410.
19. Enquist, M., and Leimar, O. (1987). Evolution of fighting behaviour: the effect of variation in resource value. *J. Theor. Biol.* 127, 187–205.
20. Enquist, M., and Leimar, O. (1990). The evolution of fatal fighting. *Anim. Behav.* 39, 1–9.
21. Smith, J.M., and Parker, G.A. (1976). The logic of asymmetric contests. *Anim. Behav.* 24, 159–175.
22. Jennions, M.D., and Backwell, P.R.Y. (1996). Residency and size affect fight duration and outcome in the fiddler crab *Uca annulipes*. *Biol. J. Linn. Soc.* 57, 293–306.
23. Panhuis, T.M., and Wilkinson, G.S. (1999). Exaggerated male eye span influences contest outcome in stalk-eyed flies (Diopsidae). *Behav. Ecol. Sociobiol.* 46, 221–227.
24. Kelly, C.D. (2006). Fighting for harems: assessment strategies during male–male contests in the sexually dimorphic Wellington tree weta. *Anim. Behav.* 72, 727–736.
25. Egge, A.R., Brandt, Y., and Swallow, J.G. (2011). Sequential analysis of aggressive interactions in the stalk-eyed fly *Teleopsis dalmani*. *Behav. Ecol. Sociobiol.* 65, 369–379.
26. Biernaskie, J.M., Grafen, A., and Perry, J.C. (2014). The evolution of index signals to avoid the cost of dishonesty. *Proc. Biol. Sci.* 281, 20140876.
27. Painting, C.J., and Holwell, G.I. (2014). Exaggerated rostra as weapons and the competitive assessment strategy of male giraffe weevils. *Behav. Ecol.* 25, 1223–1232.
28. Chen, Z.Y., Lin, C.P., and Hsu, Y. (2022). Stag beetle *Cyclommatus mniszechi* employs both mutual-and self-assessment strategies in male–male combat. *Behav. Processes* 202, 104750.
29. Palaoro, A.V., and Peixoto, P.E.C. (2022). The hidden links between animal weapons, fighting style, and their effect on contest success: a meta-analysis. *Biol. Rev. Camb. Philos. Soc.* 97, 1948–1966.

30. Berglund, A., Bisazza, A., and Pilastro, A. (1996). Armaments and ornaments: an evolutionary explanation of traits of dual utility. *Biol. J. Linn. Soc.* **58**, 385–399.
31. Hardy, I.C., and Briffa, M. (2013). *Animal Contests* (Cambridge University Press).
32. Dennenmoser, S., and Christy, J.H. (2013). The design of a beautiful weapon: compensation for opposing sexual selection on a trait with two functions. *Evolution* **67**, 1181–1188.
33. McCullough, E.L., Miller, C.W., and Emlen, D.J. (2016). Why sexually selected weapons are not ornaments. *Trends Ecol. Evol.* **31**, 742–751.
34. Levinton, J.S., and Allen, B.J. (2005). The paradox of the weakening combatant: trade-off between closing force and gripping speed in a sexually selected combat structure. *Funct. Ecol.* **19**, 159–165.
35. O'Brien, D.M., and Boisseau, R.P. (2018). Overcoming mechanical diversity in extreme hindleg weapons. *PLoS One* **13**, e0206997.
36. Levinton, J.S., and Arena, B. (2021). Direct and biometrical estimates of the closing force of major claws of the sand fiddler crab *Leptuca pugilator* (Bosc, 1801) (Decapoda: Brachyura: Ocypodidae): Support for the weakening combatant hypothesis. *J. Crustac. Biol.* **41**, ruab007.
37. Vogel, S. (2013). *Comparative Biomechanics: Life's Physical World* (Princeton University Press).
38. Goyens, J., Dirckx, J., Dierick, M., Van Hoorebeke, L., and Aerts, P. (2014). Biomechanical determinants of bite force dimorphism in *Cyclommatus metallifer* stag beetles. *J. Exp. Biol.* **217**, 1065–1071.
39. Goyens, J., Dirckx, J., and Aerts, P. (2016). Jaw morphology and fighting forces in stag beetles. *J. Exp. Biol.* **219**, 2955–2961.
40. Mills, M.R., Nemri, R.S., Carlson, E.A., Wilde, W., Gotoh, H., Lavine, L.C., and Swanson, B.O. (2016). Functional mechanics of beetle mandibles: honest signaling in a sexually selected system. *J. Exp. Zool. A Ecol. Genet. Physiol.* **325**, 3–12.
41. Levinton, J.S., and Judge, M.L. (1993). The relationship of closing force to body size for the major claw of *Uca pugnax* (Decapoda: Ocypodidae). *Funct. Ecol.* **7**, 339–345.
42. O'Brien, D.M., Boisseau, R.P., Duell, M., McCullough, E., Powell, E.C., Somjee, U., Solie, S., Hickey, A.J., Holwell, G.I., Painting, C.J., et al. (2019). Muscle mass drives cost in sexually selected arthropod weapons. *Proc. Biol. Sci.* **286**, 20191063.
43. Burrows, M., and Wolf, H. (2002). Jumping and kicking in the false stick insect *Prosatrphia teretirostris*: kinematics and motor control. *J. Exp. Biol.* **205**, 1519–1530.
44. Waltzek, T.B., and Wainwright, P.C. (2003). Functional morphology of extreme jaw protrusion in Neotropical cichlids. *J. Morphol.* **257**, 96–106.
45. McHenry, M.J. (2011). There is no trade-off between speed and force in a dynamic lever system. *Biol. Lett.* **7**, 384–386.
46. Sutton, G.P., and Burrows, M. (2011). Biomechanics of jumping in the flea. *J. Exp. Biol.* **214**, 836–847.
47. McCullough, E.L. (2014). Mechanical limits to maximum weapon size in a giant rhinoceros beetle. *Proc. Biol. Sci.* **281**, 20140696.
48. Westneat, M.W. (2004). Evolution of levers and linkages in the feeding mechanisms of fishes. *Integr. Comp. Biol.* **44**, 378–389.
49. Swanson, B.O., George, M.N., Anderson, S.P., and Christy, J.H. (2013). Evolutionary variation in the mechanics of fiddler crab claws. *BMC Evol. Biol.* **13**, 137.
50. Buchalski, B., Gutierrez, E., Emlen, D., Lavine, L., and Swanson, B. (2019). Variation in an extreme weapon: horn performance differences across rhinoceros beetle (*Trypoxylus dichotomus*) populations. *Insects* **10**, 346.
51. Palaoro, A.V., Peixoto, P.E.C., Benso-Lopes, F., Boligon, D.S., and Santos, S. (2020). Fight intensity correlates with stronger and more mechanically efficient weapons in three species of *Aegla* crabs. *Behav. Ecol. Sociobiol.* **74**, 1–11.
52. Linnaeus, C. (1771). *Mantissa Plantarum altera Generum Editiones VI. Et Specierum Edition II. Laurentii Salvii, Holamiae* (BHL).
53. Plaistow, S.J., Tsuchida, K., Tsubaki, Y., and Setsuda, K. (2005). The effect of a seasonal time constraint on development time, body size, condition, and morph determination in the horned beetle *Allomyrina dichotoma* L. (Coleoptera: Scarabaeidae). *Ecol. Entomol.* **30**, 692–699.
54. Iguchi, Y. (2006). Are beetle horns costly to produce? *Evol. Ecol. Res.* **8**, 1129–1137.
55. Hongo, Y. (2007). Evolution of male dimorphic allometry in a population of the Japanese horned beetle *Trypoxylus dichotomus septentrionalis*. *Behav. Ecol. Sociobiol.* **62**, 245–253.
56. Kojima, W., Nakakura, T., Fukuda, A., Lin, C.P., Harada, M., Hashimoto, Y., Kawachi, A., Suhama, S., and Yamamoto, R. (2020). Latitudinal cline of larval growth rate and its proximate mechanisms in a rhinoceros beetle. *Funct. Ecol.* **34**, 1577–1588.
57. Del Sol, J.F., Hongo, Y., Boisseau, R.P., Berman, G.H., Allen, C.E., and Emlen, D.J. (2021). Population differences in the strength of sexual selection match relative weapon size in the Japanese rhinoceros beetle, *Trypoxylus dichotomus* (Coleoptera: Scarabaeidae). *Evolution* **75**, 394–413.
58. Siva-Jothy, M.T. (1987). Mate securing tactics and the cost of fighting in the Japanese horned beetle, *Allomyrina dichotoma* L. (Scarabaeidae). *J. Ethol.* **5**, 165–172.
59. Setsuda, K.I., Tsuchida, K., Watanabe, H., Kakei, Y., and Yamada, Y. (1999). Size dependent predatory pressure in the Japanese horned beetle, *Allomyrina dichotoma* L. (Coleoptera: Scarabaeidae). *J. Ethol.* **17**, 73–77.
60. McCullough, E.L., Weingarten, P.R., and Emlen, D.J. (2012). Costs of elaborate weapons in a rhinoceros beetle: how difficult is it to fly with a big horn? *Behav. Ecol.* **23**, 1042–1048.
61. McCullough, E.L. (2013). Using radio telemetry to assess movement patterns in a giant rhinoceros beetle: are there differences among majors, minors, and females? *J. Insect Behav.* **26**, 51–56.
62. Obata, S., and Hidaka, T. (1983). Recognition of opponent and mate in Japanese horned beetle, *Allomyrina dichotoma* L. (Coleoptera, Scarabaeidae). *Kontyû* **51**, 534–538.
63. Karino, K., Niizuma, H., and Chiba, M. (2005). Horn length is the determining factor in the outcomes of escalated fights among male Japanese horned beetles, *Allomyrina dichotoma* L. (Coleoptera: Scarabaeidae). *J. Insect Behav.* **18**, 805–815.
64. McCullough, E.L., and Zinna, R.A. (2013). Sensilla density corresponds to the regions of the horn most frequently used during combat in the giant rhinoceros beetle *Trypoxylus dichotomus* (Coleoptera: Scarabaeidae: Dynastinae). *Ann. Entomol. Soc. Am.* **106**, 518–523. <https://doi.org/10.1603/AN12155>.
65. McCullough, E.L., Tobalske, B.W., and Emlen, D.J. (2014). Structural adaptations to diverse fighting styles in sexually selected weapons. *Proc. Natl. Acad. Sci. USA* **111**, 14484–14488.
66. Hongo, Y. (2006). Bark-carving behavior of the Japanese horned beetle *Trypoxylus dichotomus septentrionalis* (Coleoptera: Scarabaeidae). *J. Ethol.* **24**, 201–204.
67. Prell, H. (1934). Beiträge zur Kenntnis der Dynastinen (XII). Beschreibungen und Bemerkungen. *Entomol. Blatter* **30**, 54–60.
68. Nagai, S. (2006). A new species and new subspecies of the genus *Trypoxylus* from Asia and a new subspecies of the genus *Beckium* from New Guinea (Coleoptera, Scarabaeidae, Dynastinae). *Gekkan-Mushi* **428**, 13–17.
69. Nagai, S. (2007). Nihon no kabutomushi Daizukan. *BE-KUWA* **22**, 8–29.
70. Adachi, N. (2017). A new subspecies of *Trypoxylus dichotomus* (Linnaeus, 1771) (Coleoptera, Scarabaeidae, Dynastinae) from Yakushima Island and Tanegashima Island, Kagoshima Prefecture, Japan. *Kogane* **20**, 11–16.
71. Yang, H., You, C.J., Tsui, C.K.M., Tembrock, L.R., Wu, Z.Q., and Yang, P. (2021). Phylogeny and biogeography of the Japanese rhinoceros beetle, *Trypoxylus dichotomus* (Coleoptera: Scarabaeidae) based on SNP markers. *Ecol. Evol.* **11**, 153–173.

72. Nakada, M., Yonekura, N., and Lambeck, K. (1991). Late Pleistocene and halocene sea- level changes in Japan: implications for tectonic histories and mantle rheology. *Palaeogeogr. Palaeoclimatol. Palaeoecol.* 85, 107–122.

73. Government of Japan (2019). Nomination of Amami-Oshima Island, TokuNoShima Island, Northern Part of Okinawa Island, and Iriomote Island for Inscription on the World Heritage List (Government of Japan).

74. Chiang, T.Y., and Schaal, B.A. (2006). Phylogeography of plants in Taiwan and the Ryukyu Archipelago. *Taxon* 55, 31–41.

75. Nakamura, K., Suwa, R., Denda, T., and Yokota, M. (2009). Geohistorical and current environmental influences on floristic differentiation in the Ryukyu Archipelago, Japan. *J. Biogeogr.* 36, 919–928.

76. Millien-Parra, V., and Jaeger, J.J. (1999). Island biogeography of the Japanese terrestrial mammal assemblages: an example of a relict fauna. *J. Biogeogr.* 26, 959–972.

77. Park, Y.C., Kitade, O., Schwarz, M., Kim, J.P., and Kim, W. (2006). Intraspecific molecular phylogeny, genetic variation and phylogeography of *Reticulitermes speratus* (Isoptera: Rhinotermitidae). *Molecules Cells* 21, 89–103.

78. Huang, J.P., and Lin, C.P. (2010). Diversification in subtropical mountains: phylogeography, Pleistocene demographic expansion, and evolution of polyphenic mandibles in Taiwanese stag beetle, *Lucanus formosanus*. *Mol. Phylogenet. Evol.* 57, 1149–1161.

79. Jin, H., Yonezawa, T., Zhong, Y., Kishino, H., and Hasegawa, M. (2016). Cretaceous origin of giant rhinoceros beetles (Dynastini; Coleoptera) and correlation of their evolution with the Pangean breakup. *Genes Genet. Syst.* 91, 209–215.

80. Hosoya, T., and Araya, K. (2010). Invasive species problem in stag beetles and rhinoceros beetles as pet insects. In *Ecology of Introduced Organisms – Adaptive Evolution into New Environments and Possible Counter Measures*, T. Muranaka, and F. Ishihama, eds. (The Society for the Study of Species Biology).

81. Huxley, J.S. (1924). Constant differential growth-ratios and their significance. *Nature* 114, 895–896.

82. Huxley, J.S. (1932). *Problems of Relative Growth* (L. MacVeagh).

83. Gould, S.J. (1966). Allometry and size in ontogeny and phylogeny. *Biol. Rev. Camb. Philos. Soc.* 41, 587–640.

84. Gould, S.J. (1977). *Ontogeny and Phylogeny* (Harvard University Press).

85. Klingenberg, C.P. (2005). Developmental constraints, modules and evolvability. In *Variation: A Central Concept in Biology*, B. Hallgrímsson, and B.K. Hall, eds. (Elsevier), pp. 219–247.

86. Voje, K.L., Hansen, T.F., Egset, C.K., Bolstad, G.H., and Pélabon, C. (2014). Allometric constraints and the evolution of allometry. *Evolution* 68, 866–885.

87. Houle, D., Jones, L.T., Fortune, R., and Sztepanacz, J.L. (2019). Why does allometry evolve so slowly? *Integr. Comp. Biol.* 59, 1429–1440.

88. Pélabon, C., Firmat, C., Bolstad, G.H., Voje, K.L., Houle, D., Cassara, J., Rouzic, A.L., and Hansen, T.F. (2014). Evolution of morphological allometry. *Ann. N. Y. Acad. Sci.* 1320, 58–75.

89. Bolstad, G.H., Cassara, J.A., Márquez, E., Hansen, T.F., van der Linde, K., Houle, D., and Pélabon, C. (2015). Complex constraints on allometry revealed by artificial selection on the wing of *Drosophila melanogaster*. *Proc. Natl. Acad. Sci. USA* 112, 13284–13289.

90. Stillwell, R.C., Shingleton, A.W., Dworkin, I., and Frankino, W.A. (2016). Tipping the scales: evolution of the allometric slope independent of average trait size. *Evolution* 70, 433–444.

91. Frankino, W.A., Zwaan, B.J., Stern, D.L., and Brakefield, P.M. (2005). Natural selection and developmental constraints in the evolution of allometries. *Science* 307, 718–720.

92. Wilkinson, G.S. (1993). Artificial sexual selection alters allometry in the stalk-eyed fly *Cyrtodiopsis dalmani* (Diptera: Diopsidae). *Genet. Res.* 62, 213–222.

93. Shingleton, A.W., Frankino, W.A., Flatt, T., Nijhout, H.F., and Emlen, D.J. (2007). Size and shape: the developmental regulation of static allometry in insects. *BioEssays* 29, 536–548.

94. Shingleton, A.W., Mirth, C.K., and Bates, P.W. (2008). Developmental model of static allometry in holometabolous insects. *Proc. Biol. Sci.* 275, 1875–1885. <https://doi.org/10.1098/rspb.2008.0227>.

95. Tang, H.Y., Smith-Caldas, M.S., Driscoll, M.V., Salhadar, S., and Shingleton, A.W. (2011). FOXO regulates organ-specific phenotypic plasticity in *Drosophila*. *PLoS Genet.* 7, e1002373.

96. Emlen, D.J., Warren, I.A., Johns, A., Dworkin, I., and Lavine, L.C. (2012). A mechanism of extreme growth and reliable signaling in sexually selected ornaments and weapons. *Science* 337, 860–864.

97. Shingleton, A.W., and Tang, H.Y. (2012). Plastic flies: the regulation and evolution of trait variability in *Drosophila*. *Fly* 6, 147–152.

98. Gotoh, H., Hust, J.A., Miura, T., Niimi, T., Emlen, D.J., and Lavine, L.C. (2015). The Fat/Hippo signaling pathway links within-disc morphogen patterning to whole-animal signals during phenotypically plastic growth in insects. *Dev. Dyn.* 244, 1039–1045.

99. Cooper, K.L. (2019). Developmental and evolutionary allometry of the mammalian limb skeleton. *Integr. Comp. Biol.* 59, 1356–1368.

100. Okada, Y., Katsuki, M., Okamoto, N., Fujioka, H., and Okada, K. (2019). A specific type of insulin-like peptide regulates the conditional growth of a beetle weapon. *PLoS Biol.* 17, e3000541.

101. Toubiana, W., Armisén, D., Viala, S., Decaras, A., and Khila, A. (2021). The growth factor BMP11 is required for the development and evolution of a male exaggerated weapon and its associated fighting behavior in a water strider. *PLoS Biol.* 19, e3001157.

102. Vea, I.M., and Shingleton, A.W. (2021). Network-regulated organ allometry: the developmental regulation of morphological scaling. *Wiley Interdiscip. Rev. Dev. Biol.* 10, e391.

103. Alatalo, R.V., Höglund, J., and Lundberg, A. (1988). Patterns of variation in tail ornament size in birds. *Biol. J. Linnaean Soc.* 34, 363–374.

104. Fitzpatrick, S. (1997). Patterns of morphometric variation in birds' tails: length, shape and variability. *Biol. J. Linnaean Soc. Lond.* 62, 145–162.

105. Kodric-Brown, A., Sibley, R.M., and Brown, J.H. (2006). The allometry of ornaments and weapons. *Proc. Natl. Acad. Sci. USA* 103, 8733–8738.

106. Cuervo, J.J., and Möller, A.P. (2009). The allometric pattern of sexually size dimorphic feather ornaments and factors affecting allometry. *J. Evol. Biol.* 22, 1503–1515.

107. Knell, R.J., Naish, D., Tomkins, J.L., and Hone, D.W. (2013). Sexual selection in prehistoric animals: detection and implications. *Trends Ecol. Evol.* 28, 38–47.

108. Hone, D.E., Wood, D., and Knell, R.J. (2016). Positive allometry for exaggerated structures in the ceratopsian dinosaur *Protoceratops andrewsi* supports socio-sexual signaling. *Palaeontol. Electron.* 19, 1–13.

109. Fromhage, L., and Kokko, H. (2014). Sexually selected traits evolve positive allometry when some matings occur irrespective of the trait. *Evolution* 68, 1332–1338.

110. Voje, K.L. (2016). Scaling of morphological characters across trait type, sex, and environment: a meta-analysis of static allometries. *Am. Nat.* 187, 89–98.

111. Eberhard, W.G., Rodríguez, R.L., Huber, B.A., Speck, B., Miller, H., Buzatto, B.A., and Machado, G. (2018). Sexual selection and static allometry: the importance of function. *Q. Rev. Biol.* 93, 207–250.

112. O'Brien, D.M., Allen, C.E., Van Kleeck, M.J., Hone, D., Knell, R., Knapp, A., Christiansen, S., and Emlen, D.J. (2018). On the evolution of extreme structures: static scaling and the function of sexually selected signals. *Anim. Behav.* 144, 95–108.

113. Rodríguez, R.L., and Eberhard, W.G. (2019). Why the static allometry of sexually- selected traits is so variable: the importance of function. *Integr. Comp. Biol.* 59, 1290–1302.

114. Hasson, O. (1991). Sexual displays as amplifiers: practical examples with an emphasis on feather decorations. *Behav. Ecol.* 2, 189–197.

115. Wallace, B. (1987). Ritualistic combat and allometry. *Am. Nat.* 129, 775–776.

116. Cotton, S., Fowler, K., and Pomiankowski, A. (2004). Do sexual ornaments demonstrate heightened condition-dependent expression as predicted by the handicap hypothesis? *Proc. Biol. Sci.* 271, 771–783.

117. Bonduriansky, R. (2007). The evolution of condition-dependent sexual dimorphism. *Am. Nat.* 169, 9–19.

118. Bradbury, J.W., and Vehrencamp, S.L. (2011). *Principles of Animal Communication*, Second Edition (Sinauer Associates, Inc.).

119. Tazzyman, S.J., Iwasa, Y., and Pomiankowski, A. (2014). Signaling efficacy drives the evolution of larger sexual ornaments by sexual selection. *Evolution* 68, 216–229.

120. Warren, I.A., Gotoh, H., Dworkin, I.M., Emlen, D.J., and Lavine, L.C. (2013). A general mechanism for conditional expression of exaggerated sexually-selected traits. *BioEssays* 35, 889–899.

121. Knell, R.J., Fruhauf, N., and Norris, K.A. (1999). Conditional expression of a sexually selected trait in the stalk-eyed fly *Diasemopsis aethiopica*. *Ecol. Entomol.* 24, 323–328.

122. David, P., Bjorksten, T., Fowler, K., and Pomiankowski, A. (2000). Condition-dependent signalling of genetic variation in stalk-eyed flies. *Nature* 406, 186–188.

123. Cotton, S., Fowler, K., and Pomiankowski, A. (2004). Condition dependence of sexual ornament size and variation in the stalk-eyed fly *Cyrtodiopsis dalmanni* (Diptera: Diopsidae). *Evolution* 58, 1038–1046.

124. Bonduriansky, R., and Rowe, L. (2005). Sexual selection, genetic architecture, and the condition dependence of body shape in the sexually dimorphic fly *Prochyliza xanthostoma* (Piophilidae). *Evolution* 59, 138–151.

125. Johns, A., Gotoh, H., McCullough, E.L., Emlen, D.J., and Lavine, L.C. (2014). Heightened condition-dependent growth of sexually selected weapons in the rhinoceros beetle, *Trypoxylus dichotomus* (Coleoptera: Scarabaeidae). *Integr. Comp. Biol.* 54, 614–621. <https://doi.org/10.1093/icb/icu041>.

126. Searcy, W.A., and Beecher, M.D. (2009). Song as an aggressive signal in songbirds. *Anim. Behav.* 78, 1281–1292.

127. Eberhard, W.G., and Garcia, C. (2000). Ritual jousting by horned *Paracoschoenus expositus* weevils (Coleoptera, Curculionidae, Baridinae). *Psyche J. Entomol.* 103, 55–84.

128. Eberhard, W.G. (1998). Sexual behavior of *Acanthocephala declivis guatemalana* (Hemiptera: Coreidae) and the allometric scaling of their modified hind legs. *Ann. Entomol. Soc. Am.* 91, 863–871.

129. Miyatake, T. (1997). Functional morphology of the hind legs as weapons for male contests in *Leptoglossus australis* (Heteroptera: Coreidae). *J. Insect Behav.* 10, 727–735.

130. Katsuki, M., Yokoi, T., Funakoshi, K., and Oota, N. (2014). Enlarged hind legs and sexual behavior with male-male interaction in *Sagra femorata* (Coleoptera: Chrysomelidae). *Entomological News* 124, 211–220.

131. McCullough, E.L., Ledger, K.J., O'Brien, D.M., and Emlen, D.J. (2015). Variation in the allometry of exaggerated rhinoceros beetle horns. *Anim. Behav.* 109, 133–140.

132. Van Noordwijk, A.J., and De Jong, G. (1986). Acquisition and allocation of resources: their influence on variation in life history tactics. *Am. Nat.* 128, 137–142.

133. Houle, D. (1991). Genetic covariance of fitness correlates: what genetic correlations are made of and why it matters. *Evolution* 45, 630–648.

134. Kotiaho, J.S. (2001). Costs of sexual traits: a mismatch between theoretical considerations and empirical evidence. *Biol. Rev. Camb. Philos. Soc.* 76, 365–376.

135. Agrawal, A.A., Conner, J.K., and Rasmann, S. (2010). Tradeoffs and negative correlations in evolutionary ecology. *Evol. Since Darwin First* 150, 243–268.

136. Garland, T., Jr., Downs, C.J., and Ives, A.R. (2022). Trade-offs (and constraints) in organismal biology. *Physiol. Biochem. Zool.* 95, 82–112.

137. Oufiero, C.E., and Garland, T., Jr. (2007). Evaluating performance costs of sexually selected traits. *Funct. Ecol.* 21, 676–689.

138. Swallow, J., and Husak, J. (2011). Compensatory traits and the evolution of male ornaments. *Behaviour* 148, 1–29.

139. Peterson, B.K., Weber, J.N., Kay, E.H., Fisher, H.S., and Hoekstra, H.E. (2012). Double digest RADSeq: an inexpensive method for *de novo* SNP discovery and genotyping in model and non-model species. *PLoS One* 7, e37135.

140. Catchen, J., Hohenlohe, P.A., Bassham, S., Amores, A., and Cresko, W.A. (2013). Stacks: an analysis tool set for population genomics. *Mol. Ecol.* 22, 3124–3140.

141. Rochette, N.C., Rivera-Colón, A.G., and Catchen, J.M. (2019). Stacks 2: Analytical methods for paired-end sequencing improve RADseq-based population genomics. *Mol. Ecol.* 28, 4737–4754.

142. Li, H. (2013). Aligning sequence reads, clone sequences and assembly contigs with BWA-MEM. <https://doi.org/10.48550/arXiv.1303.3997>.

143. Li, H. (2011). A statistical framework for SNP calling, mutation discovery, association mapping and population genetic parameter estimation from sequencing data. *Bioinformatics* 27, 2987–2993.

144. Li, H., Handsaker, B., Wysoker, A., Fennell, T., Ruan, J., Homer, N., Marth, G., Abecasis, G., and Durbin, R.; 1000 Genome Project Data Processing Subgroup (2009). The sequence alignment/map format and SAMtools. *Bioinformatics* 25, 2078–2079.

145. Alexander, D.H., Novembre, J., and Lange, K. (2009). Fast model-based estimation of ancestry in unrelated individuals. *Genome Res.* 19, 1655–1664.

146. Bouckaert, R., Heled, J., Kühnert, D., Vaughan, T., Wu, C.H., Xie, D., Suchard, M.A., Rambaut, A., and Drummond, A.J. (2014). BEAST 2: a software platform for Bayesian evolutionary analysis. *PLoS Comp. Biol.* 10, e1003537.

147. Rambaut, A., Drummond, A.J., Xie, D., Baele, G., and Suchard, M.A. (2018). Posterior summarization in Bayesian phylogenetics using Tracer 1.7. *Syst. Biol.* 67, 901–904.

148. Bouckaert, R.R., and Heled, J. (2014). DensiTree 2: Seeing trees through the forest. *bioRxiv*, 012401.

149. Drummond, A.J., and Rambaut, A. (2007). BEAST: bayesian evolutionary analysis by sampling trees. *BMC Evol. Biol.* 7, 214.

150. Rambaut, A. (2017). FigTree-version 1.4. 3, a graphical viewer of phylogenetic trees. Computer Program Distributed by the Author. <http://tree.bio.ed.ac.uk/software/figtree>.

151. R Core Team (2019). R: A Language and Environment for Statistical Computing (R Foundation for Statistical Computing). <https://www.R-project.org/>.

152. Lenth, R. (2023). Emmeans: estimated marginal means, aka least-squares means. R package version 1.8.7. <https://cran.r-project.org/web/packages/emmeans/index.html>.

153. Pinheiro, J., and Bates, D.; R Core Team (2023). Nlme: linear and nonlinear mixed effects models. R package version 3.1-162. <https://CRAN.R-project.org/package=nlme>.

154. Benjamini, Y., and Hochberg, Y. (1995). Controlling the false discovery rate: a practical and powerful approach to multiple testing. *J. R. Stat. Soc. B* 57, 289–300.

155. Laurent, E.L. (2000). Children, “insects” and play in Japan. In *Companion Animals and Us: Exploring the Relationships between People and Pets* (Cambridge University Press), pp. 61–89.

156. Kawahara, A.Y. (2007). Thirty-foot telescopic nets, bug-collecting video games, and beetle pets: entomology in modern Japan. *Am. Entomol.* 53, 160–172.

157. Brock, R.L. (2006). Insect fads in Japan and collecting pressure on New Zealand insects. *The Weta* 32, 7–15.

158. Takada, K. (2013). Exploitation of flagship species of scarabaeid beetles with application of analyzed results on cultural entomology. *Appl. Ecol. Environ. Sci.* 1, 1–6.

159. Rowland, J.M., and Miller, K.B. (2012). Phylogeny and systematics of the giant rhinoceros beetles (Scarabaeidae: Dynastini). *Insecta Mundi* 263, 1–15.

160. Dutrillaux, A.-M., Mamuris, Z., and Dutrillaux, B. (2013). Chromosome analyses challenge the taxonomic position of *Augosoma centaurus* Fabricius, 1775 (Coleoptera: Scarabaeidae: Dynastinae) and the separation of Dynastini and Oryctini. *Zoosystema* 35, 537–549. <https://doi.org/10.5252/z2013>.

161. Kôno, H. (1931). Die *Trypoxylus*-Arten aus Japan und Formosa (Col. Scarabaeidae). *Insecta Matsumurana* 5, 159–160.

162. Kusui, Y. (1976). Notes on the *Allomyrina dichotoma* (Linne) from Okinawa islands (Coleoptera, Scarabaeidae). *Entomol. Rev. Jpn.* 29, 51–54.

163. Satoru, T. (2014). A new subspecies of *Trypoxylus dichotomus* (Coleoptera: Scarabaeidae: Dynastinae) from China. *Indian J. Entomol.* 76, 149–151.

164. Bayona-Vásquez, N.J., Glenn, T.C., Kieran, T.J., Pierson, T.W., Hoffberg, S.L., Scott, P.A., Bentley, K.E., Finger, J.W., Louha, S., Troendle, N., et al. (2019). Adapterama III: Quadruple-indexed, double/triple-enzyme RADseq libraries (2rad/3rad). *PeerJ* 7, e7724, <https://doi.org/10.7717/peerj.7724>.

165. Morita, S., Ando, T., Maeno, A., Mizutani, T., Mase, M., Shigenobu, S., and Niimi, T. (2019). Precise staging of beetle horn formation in *Trypoxylus dichotomus* reveals the pleiotropic roles of doublesex depending on the spatiotemporal developmental contexts. *PLoS Genet.* 15, e1008063.

166. Bryant, D., Bouckaert, R., Felsenstein, J., Rosenberg, N.A., and RoyChoudhury, A. (2012). Inferring species trees directly from biallelic genetic markers: bypassing gene trees in a full coalescent analysis. *Mol. Biol. Evol.* 29, 1917–1932.

167. Baker, R.H., and Wilkinson, G.S. (2001). Phylogenetic analysis of sexual dimorphism and eye-span allometry in stalk-eyed flies (Diopsidae). *Evolution* 55, 1373–1385.

168. Tomkins, J.L. (1999). Environmental and genetic determinants of the male forceps length dimorphism in the European earwig *Forficula auricularia* L. *Behav. Ecol. Sociobiol.* 47, 1–8.

169. Tomkins, J.L., and Brown, G.S. (2004). Population density drives the local evolution of a threshold dimorphism. *Nature* 431, 1099–1103.

170. Emlen, D.J. (1994). Environmental control of horn length dimorphism in the beetle *Onthophagus acuminatus* (Coleoptera: Scarabaeidae). *Proc. R. Soc. Lond. B* 256, 131–136.

171. Emlen, D.J. (1996). Artificial selection on horn length–body size allometry in the horned beetle *Onthophagus acuminatus* (Coleoptera: Scarabaeidae). *Evolution* 50, 1219–1230.

172. Moczek, A.P., and Emlen, D.J. (1999). Proximate determination of male horn dimorphism in the beetle *Onthophagus taurus* (Coleoptera: Scarabaeidae). *J. Evol. Biol.* 12, 27–37.

173. Okada, K., and Miyatake, T. (2009). Genetic correlations between weapons, body shape and fighting behaviour in the horned beetle *Gnatocerus cornutus*. *Anim. Behav.* 77, 1057–1065.

174. Okada, K., and Miyatake, T. (2010). Effect of losing on male fights of broad-horned flour beetle, *Gnatocerus cornutus*. *Behav. Ecol. Sociobiol.* 64, 361–369.

175. O'Brien, D.M., Katsuki, M., and Emlen, D.J. (2017). Selection on an extreme weapon in the frog-legged leaf beetle (*Sagra femorata*). *Evolution* 71, 2584–2598.

176. Karino, K., Seki, N., and Chiba, M. (2004). Larval nutritional environment determines adult size in Japanese horned beetles *Allomyrina dichotoma*. *Ecol. Res.* 19, 663–668.

177. Ito, Y., Harigai, A., Nakata, M., Hosoya, T., Araya, K., Oba, Y., Ito, A., Ohde, T., Yaginuma, T., and Niimi, T. (2013). The role of doublesex in the evolution of exaggerated horns in the Japanese rhinoceros beetle. *EMBO Rep.* 14, 561–567.

178. Adachi, H., Matsuda, K., Niimi, T., Kondo, S., and Gotoh, H. (2020). Genetical control of 2D pattern and depth of the primordial furrow that prefigures 3D shape of the rhinoceros beetle horn. *Sci. Rep.* 10, 18687.

179. Ohde, T., Morita, S., Shigenobu, S., Morita, J., Mizutani, T., Gotoh, H., Zinna, R.A., Nakata, M., Ito, Y., Wada, K., et al. (2018). Rhinoceros beetle horn development reveals deep parallels with dung beetles. *PLoS Genet.* 14, e1007651.

180. Emlen, D.J., and Allen, C.E. (2003). Genotype to phenotype: physiological control of trait size and scaling in insects. *Integr. Comp. Biol.* 43, 617–634.

181. Emlen, D.J., and Nijhout, H.F. (2000). The development and evolution of exaggerated morphologies in insects. *Annu. Rev. Entomol.* 45, 661–708.

182. Dreyer, A.P., Saleh Ziabari, O.S., Swanson, E.M., Chawla, A., Frankino, W.A., and Shingleton, A.W. (2016). Cryptic individual scaling relationships and the evolution of morphological scaling. *Evolution* 70, 1703–1716.

183. Iguchi, Y. (2002). Further evidence of male trimorphism in the horned beetle *Trypoxylus dichotomus septentrionalis* (Coleoptera, Scarabaeidae). *Bull. Japan. Soc. Coleopterol.* 5, 319–322.

184. Knell, R.J. (2009). On the analysis of non-linear allometries. *Ecol. Entomol.* 34, 1–11.

185. Packard, G.C. (2021). Is allometric variation in the cephalic horn on male rhinoceros beetles discontinuously dimorphic? *Evol. Biol.* 48, 233–245.

186. Parzer, H.F., and Moczek, A.P. (2008). Rapid antagonistic coevolution between primary and secondary sexual characters in horned beetles. *Evolution* 62, 2423–2428.

187. Casasa, S., and Moczek, A.P. (2018). The role of ancestral phenotypic plasticity in evolutionary diversification: population density effects in horned beetles. *Anim. Behav.* 137, 53–61.

188. Raffalovich, L.E., Deane, G.D., Armstrong, D., and Tsao, H.S. (2008). Model selection procedures in social research: Monte-Carlo simulation results. *J. Appl. Stat.* 35, 1093–1114.

189. Link, W.A., and Barker, R.J. (2006). Model weights and the foundations of multi-model inference. *Ecology* 87, 2626–2635.

190. Galipaud, M., Gillingham, M.A.F., David, M., and Dechaume-Moncharmont, F.X. (2014). Ecologists overestimate the importance of predictor variables in model averaging: a plea for cautious interpretations. *Methods Ecol. Evol.* 5, 983–991.

191. Nakagawa, S. (2004). A farewell to Bonferroni: the problems of low statistical power and publication bias. *Behav. Ecol.* 15, 1044–1045.

192. Onofri, A. (2020). The broken bridge between biologists and statisticians: a blog and R package, Statforbiology. Italianist, web. <https://www.statforbiology.com>.

193. Schneider, C.A., Rasband, W.S., and Eliceiri, K.W. (2012). NIH Image to ImageJ: 25 years of image analysis. *Nat. Methods* 9, 671–675. <https://doi.org/10.1038/nmeth.2089>.

194. Engqvist, L. (2005). The mistreatment of covariate interaction terms in linear model analyses of behavioural and evolutionary ecology studies. *Anim. Behav.* 70, 967–971.

STAR★METHODS

KEY RESOURCES TABLE

REAGENT or RESOURCE	SOURCE	IDENTIFIER
<b>Biological samples</b>		
Adult <i>Allomyrina pfeifferii</i> (Philippines) (n=14 individuals)	Wild caught for this study	Ap
Adult <i>Xyloscaptes davidis</i> (Thailand) (n=9)	Wild caught for this study	Xd/davidus
Adult <i>Trypoxylus dichotomus septentrionalis</i> (Kyoto, Japan) (n=14)	Wild caught for this study	K
Adult <i>Trypoxylus dichotomus septentrionalis</i> (Matsuzaka, Japan) (n=16)	Wild caught for this study	M
Adult <i>Trypoxylus dichotomus septentrionalis</i> (Okazaki, Japan) (n=18)	Wild caught for this study	Oi
Adult <i>Trypoxylus dichotomus septentrionalis</i> (Hamamatsu, Japan) (n=9)	Wild caught for this study	Ham
Adult <i>Trypoxylus dichotomus septentrionalis</i> (Kyushu, Japan) (n=12)	Wild caught for this study	Fuk
Adult <i>Trypoxylus dichotomus septentrionalis</i> (Goto island, Japan) (n=12)	Wild caught for this study	Goto
Adult <i>Trypoxylus dichotomus tsuchiyai</i> (Kuchinoerabu Island, Japan) (n=8)	Wild caught for this study	Kuch
Adult <i>Trypoxylus dichotomus shizue</i> (Tanegashima island, Japan) (n=19)	Wild caught for this study	Tan
Adult <i>Trypoxylus dichotomus shizue</i> (Yakushima island, Japan) (n=10)	Wild caught for this study	Yak
Adult <i>Trypoxylus kanamorii</i> (Myanmar/Thailand) (n=7)	Wild caught for this study	Kan
Adult <i>Trypoxylus dichotomus politus</i> (Chiang Mai, Thailand) (n=4)	Wild caught for this study	Thai
Adult <i>Trypoxylus dichotomus inchachina</i> (Kumejima, Japan) (n=6)	Wild caught for this study	KUM
Adult <i>Trypoxylus dichotomus takarei</i> (Okinawa Island, Japan) (n=13)	Wild caught for this study	OK/Oki/Oa
Adult <i>Trypoxylus dichotomus dichotomus</i> (Fuzhou city, China) (n=9)	Wild caught for this study	FF
Adult <i>Trypoxylus dichotomus dichotomus</i> (Jiulingshan, China) (n=9)	Wild caught for this study	JJ
Adult <i>Trypoxylus dichotomus dichotomus</i> (Lianhuashan, China) (n=10)	Wild caught for this study	LG
Adult <i>Trypoxylus dichotomus dichotomus</i> (Shantou city, China) (n=10)	Wild caught for this study	SG
Adult <i>Trypoxylus dichotomus dichotomus</i> (Wuyishan, China) (n=10)	Wild caught for this study	WJ
Adult <i>Trypoxylus dichotomus dichotomus</i> (Xiamen city, China) (n=10)	Wild caught for this study	XF
Adult <i>Trypoxylus dichotomus dichotomus</i> (Zhugangshan, China) (n=10)	Wild caught for this study	ZH
Adult <i>Trypoxylus dichotomus tsunobosonus</i> (Puli, Taiwan) (n=20)	Wild caught for this study	Taiw2
Adult <i>Trypoxylus dichotomus tsunobosonus</i> (Chiayi, Taiwan) (n=13)	Wild caught for this study	Taiw1/CH

(Continued on next page)

**Continued**

REAGENT or RESOURCE	SOURCE	IDENTIFIER
Adult <i>Trypoxylus dichotomus tsunobosonus</i> (Taiwan) (n=10)	Wild caught for this study	Taiw3/TP
<b>Chemicals, peptides, and recombinant proteins</b>		
Wizard SV Genomic DNA purification kit	Promega	Cat # A1120
PicoGreen dsDNA kit	Thermo Fisher Scientific (Life technologies)	Cat # P7589
NlaIII restriction enzyme	New England Biolabs	Cat # R0125S
MluCI restriction enzyme	New England Biolabs	Cat # R0538S
Cytiva Sera-Mag SpeedBeads	Fisher scientific	Cat # 09-981-123
Pippin Prep 2% Agarose Gel Cassette	Sage Science	Cat # HTC2010
Dynabeads M-270 Streptavidin	Thermo Fisher Scientific	Cat # 65305
Phusion High Fidelity PCR kit	New England Biolabs	Cat # E0553L
<b>Deposited data</b>		
Illumina HiSeq ddRAD-seq Sequencing	This paper	NCBI SRA BioProject Accession: PRJNA1003128
Morphological measurements	This paper	<a href="https://osf.io/dc2fx/">https://osf.io/dc2fx/</a>
<b>Oligonucleotides</b>		
Ligation adapter P1	Peterson et al. <sup>139</sup>	SphI-compatible
Ligation adapter P2	Peterson et al. <sup>139</sup>	MluCI compatible with NNNNNIII barcode for PCR duplicate removal
<b>Software and algorithms</b>		
Stacks (version 1.13)	Catchen et al. <sup>140</sup> ; Rochette et al. <sup>141</sup>	<a href="https://catchenlab.life.illinois.edu/stacks/">https://catchenlab.life.illinois.edu/stacks/</a>
PCR duplicates removal and R statistics script	This paper	<a href="https://osf.io/dc2fx/">https://osf.io/dc2fx/</a>
BWA MEM (0.7.12)	Li <sup>142</sup>	<a href="https://bio-bwa.sourceforge.net/bwa.shtml">https://bio-bwa.sourceforge.net/bwa.shtml</a>
SAMtools (version 1.5)	Li <sup>142,143</sup> ; Li et al. <sup>144</sup>	<a href="http://www.htslib.org/doc/1.5/samtools.html">http://www.htslib.org/doc/1.5/samtools.html</a>
ADMIXTURE (1.3.0)	Alexander et al. <sup>145</sup>	<a href="https://dalexander.github.io/admixture/">https://dalexander.github.io/admixture/</a>
BEAST (version 2.4.5)	Bouckaert et al. <sup>146</sup>	<a href="https://www.beast2.org/">https://www.beast2.org/</a>
Tracer (version 1.7)	Rambaut et al. <sup>147</sup>	<a href="https://beast.community/tracer">https://beast.community/tracer</a>
DensiTree (2.2.3)	Bouckaert and Heled <sup>148</sup>	<a href="https://www.cs.auckland.ac.nz/~remco/DensiTree/">https://www.cs.auckland.ac.nz/~remco/DensiTree/</a>
TreeAnnotator (1.10)	Drummond and Rambaut <sup>149</sup>	<a href="https://www.beast2.org/treeannotator/">https://www.beast2.org/treeannotator/</a>
FigTree (1.44)	Rambaut <sup>150</sup>	<a href="http://tree.bio.ed.ac.uk/software/figtree/">http://tree.bio.ed.ac.uk/software/figtree/</a>
R (version 4.1.1)	R Core Team <sup>151</sup>	<a href="https://www.r-project.org/">https://www.r-project.org/</a>
emmeans (R package, version 1.8.7)	Lenth <sup>152</sup>	<a href="https://cran.r-project.org/web/packages/emmeans/index.html">https://cran.r-project.org/web/packages/emmeans/index.html</a>
nlme (R package, version 3.1-162)	Pinheiro et al. <sup>153</sup>	<a href="https://CRAN.R-project.org/package=nlme">https://CRAN.R-project.org/package=nlme</a>
aomisc (R package, version 0.650)	Benjamini and Hochberg <sup>154</sup>	<a href="https://github.com/OnofriAndreaPG/aomisc">https://github.com/OnofriAndreaPG/aomisc</a>

**RESOURCE AVAILABILITY**

**Lead contact**

Requests for further information and resources should be directed to and will be fulfilled by [doug.emlen@mso.umt.edu](mailto:doug.emlen@mso.umt.edu).

**Materials availability**

This study did not generate new unique reagents.

**Data and code availability**

- The data that support the findings of this study are available from the corresponding author(s) upon reasonable request. DNA sequence data are deposited in the NCBI Short Read Archive, BioProject SRA: PRJNA1003128.

- This paper reports original codes available from the authors upon reasonable request or have been uploaded on OSF (<https://osf.io/dc2fx/>)
- Any additional information required to reanalyze the data reported in this paper is available from the lead contact upon request.

## EXPERIMENTAL MODEL AND SUBJECT DETAILS

Japanese rhinoceros beetles ('Yamato kabutomushi') are large, abundant, and often observed scarabs native to Eastern Asia, including mainland China, Taiwan, Korea and Japan.<sup>155–158</sup> Males have a short, curved horn extending from the dorsal prothorax and a much longer, four-tined "pitchfork" shaped horn extending from the top of the head (Figure 2). Males of the two closest sister species, *Xylocaptes davidis* and *Allomyrina pfeifferi*,<sup>71,79,159,160</sup> have a much smaller, two-tined forked horn extending from the center of the head. Both *X. davidis* and *A. pfeifferi* are rare and very poorly understood outside of systematics.

Ten subspecies of *T. dichotomus* have been described based on geographic location and morphology, including conspicuous and consistent population differences in relative horn length (*T. d. septentrionalis* [Korean Peninsula, Japan<sup>69,161</sup>]; *T. d. tsuchiyai* [Kuchi-noerabu Island<sup>69</sup>]; *T. d. shizuae* [Yakushima and Tanegashima Islands<sup>70</sup>]; *T. d. dichotomus* [Mainland China; Linnaeus 1771, Nagai 2007]; *T. d. tsunobosonus* [Taiwan<sup>69,161</sup>]; *T. d. takarai* [Okinawa<sup>162</sup>]; *T. d. inchachina* [Kumejima<sup>162</sup>]; *T. d. politus* [Myanmar, Thailand, Vietnam<sup>67,69</sup>]; *T. d. shennongjii* [Shennongjii, Hubei, China<sup>163</sup>]; and *T. kanamorii* [Myanmar<sup>68</sup>]).

## METHOD DETAILS

Our approach comprised the following steps, each described in detail below: (1) samples of wild animals were collected from 23 locations across the range of the species and including 9 of the 10 described subspecies (Table S1); (2) genomic DNA was extracted from approximately 10 animals per location (198 beetles total) and sequenced to identify approximately 13,500 informative SNPs distributed across the genome; (3) we assigned animals from the different locations to 9 genetically and morphologically distinguishable populations; (4) two individuals from each of these populations and from the outgroup *X. davidis* were then used to perform coalescent analyses of population ancestry, generating a well-supported phylogeny for the historical relationships among the populations; animals from all of the sample localities were then pooled into their respective genetic populations and these groupings were used for morphological comparisons of relative horn length (4) and for biomechanical calculations of horn strength (5).

Once the genetic populations had been defined, we added additional samples (n = 1375) from these same regions to increase our sample sizes for the horn length versus body size allometry estimation, and to improve our ability to test for differences in relative horn length across populations. Because these additional animals were from private collections we did not use them for the biomechanical force estimation, which would have required destructive sampling of the specimens.

### DNA extraction and ddRAD library preparation

For DNA extraction, we removed cuticle and isolated ~20mg of muscle tissue from each individual sample, then performed tissue lysis and DNA isolation using the Wizard SV Genomic DNA Purification kit (Promega). We fluorometrically quantified DNA using the PicoGreen dsDNA kit (Life Technologies) and constructed double digest restriction-site associated DNA sequencing libraries for Illumina Sequencing following Peterson et al.<sup>139</sup> Briefly, after normalizing samples to 15, 30 or 90 ng, we performed double restriction digests using the enzymes NlallI and MluCI (New England Biolabs). All enzymatic steps were followed by cleanups with solid-phase reversible immobilization beads (Sera-mag Speedbeads, Fisher). Post digest, we performed ligations with adapters P1 and P2, pooled samples (<48 samples per pool), and ran each pool on one lane of a Pippin Prep 2% agarose MarkerB 100–600 bp Gel Cassette (Sage Science) to collect fragments between 426–462bp in length, which includes additional adapter sequences. We then enriched for fragments ligated to P2 adapters using streptavidin-coupled beads (Dynabeads M-270, Invitrogen). Finally, we amplified each pool using 4 separate PCRs, each with 12-cycles (Phusion High Fidelity PCR kit, New England Biolabs).

### Mapping and genotyping

All libraries were sequenced using 2x150bp reads on an Illumina HiSeq 4000 machine. After sequencing, we demultiplexed raw reads by individuals using the "process\_radtags" function in Stacks version 1.13.<sup>140,141</sup> We next removed PCR duplicates (facilitated by a unique molecular index located on the i7 index read<sup>164</sup> and a custom python script) and mapped reads to a draft *T. dichotomus* genome<sup>165</sup> using BWA-MEM.<sup>142</sup> We calculated genotype probabilities using the mpileup algorithm (options: flags -C 50, -E, -S, -D, -u, -l) and performed genotype calls using BCFtools, with both functions available in the SAMtools package (Version 1.5<sup>143,144</sup>).

After examining several measures of read depth and quality, we implemented an initial filter to retain only genotypes with a minimum per individual depth of 8 and minimum genotype quality of 30, and only kept sites where the mean depth was greater than 1. We next removed any sites where less than 50% of individuals had genotype calls. We further removed 500bp windows (i.e., full RAD-tags) containing more than six SNPs with high depth reads (>1000), as well as any regions containing SNPs with total depth >1300. Additional filters specific to different analyses are noted when appropriate in the following sections.

## QUANTIFICATION AND STATISTICAL ANALYSIS

### Population genetic analyses

We used a cross validation approach implemented in the software package ADMIXTURE<sup>145</sup> to estimate the number of population clusters. Because high LD can lead to spurious signals, we first thinned our dataset by identifying any SNPs located within 50bp of each other and having an  $R^2$  value  $> 0.1$ , and then only keeping the site with the highest minor allele frequency. For the ADMIXTURE runs, we tested subpopulation (k) values ranging from four to nine, and determined the best model fit by identifying the k value that minimized CV error.

### Coalescent Analyses and Phylogeny Construction

We estimated phylogeny using beetles collected from 16 of our 23 sample locations, representing all of the genetically distinguishable populations identified by the ADMIXTURE analyses and all 9 of the formally described subspecies included in this study (key resources table). Specifically, we compiled genotype data for two beetles from each of the 16 sample locations, keeping individuals with the most complete genotype coverage in each population, as well as one outgroup individual from the sister species *Xyloscaptus davidis*. We then estimated population ancestry using a full coalescent analysis (SNAPP<sup>166</sup>) implemented in BEAST v2.4.5.<sup>146</sup> For the SNAPP analysis, we used a gamma rate prior, used the built-in function to estimate mutation rates U and V, and ran the MCMC for up to 2 million cycles, storing data every 1,000 cycles. All other parameters were run with default settings. Runs were continued until the estimated sample size (ESS) for the posterior probabilities exceeded a value of 200. ESS's for other model parameters were also evaluated with the Tracer v1.7 software.<sup>147</sup>

We first ran a full tree using all of the genetically distinguishable *T. dichotomus* populations (sixteen of the sample locations) and *X. davidis* as an outgroup. This tree revealed a well-supported deep split between northern and southern *Trypoxylus* lineages, suggesting the beetles colonized these regions independently with each clade having its own evolutionary trajectories. However, our DNA from *X. davidis* was degraded relative to our other samples, reducing the number of usable SNPs. We therefore ran separate, clade-specific analyses for these northern and southern trees, using a representative from the other clade as an outgroup instead of *X. davidis*, increasing the number of usable SNPs from 747 to 2,093 and 4,091 respectively.

The northern analysis included a total of 6 locations (Kyushu, Kyoto, Matsuzaka, Hamamatsu, Yakushima Island and Tanegashima Island) and Wuyishan, China, as an outgroup, while the southern analysis used 5 locations (*T. kanamorii* [Myanmar]; *T. d. politus* [Thailand]; Okinawa, Fuzhou City, and Taiwan) and Matsuzaka, Japan, as an outgroup. Finally, we sampled from the resulting tree files, after removing the first 10% of traces as a burn-in, to estimate branch lengths and generate posterior probabilities for all nodes. Tree annotation and visualization was performed using the Densitree<sup>148</sup> and TreeAnnotator<sup>149</sup> software supplied with BEAST2, as well as FigTree.<sup>150</sup>

### Weapon Size Comparisons

As in other insect taxa with highly plastic sexually selected structures (e.g., fly eyestalks<sup>92,121,122,167</sup>; earwig forceps<sup>168,169</sup>; dung beetle horns<sup>170–172</sup>; flour beetle mandibles<sup>173,174</sup>; frog-legged leaf beetle hindlegs<sup>175</sup>), *Trypoxylus* horn length *per se* has little detectable heritability in contemporary populations<sup>125,176</sup> and horn length evolution likely arises through changes in the developmental mechanisms modulating horn growth in relation to the nutritional state and overall body size of an animal.<sup>96,98,165,177–179</sup> Therefore, we compare relative sizes of horns across populations by comparing the steepness, elevation, and/or shape of population-level patterns of horn length / body size scaling.<sup>93,175,180–182</sup>

All statistical analyses were performed in R (version 4.1.1<sup>151</sup>). For all models assuming normally distributed and homoscedastic errors, we systematically checked and confirmed this assumption by plotting the residuals against normal quantiles and residual vs fitted values. We first compared the horn length / body size scaling relationships between the outgroup *X. davidis* and the northern and southern *T. dichotomus* clades. We fitted a linear mixed model (function lme, R package “nlme<sup>153</sup>”) including  $\log_{10}$  horn length as the response variable and  $\log_{10}$  thorax width, lineage, and their interaction as fixed effects. The population of origin was included as a random effect. Significance of the fixed effects was assessed using a type I (sequential) ANCOVA. This allowed us to test for differences between major clades in relative horn length, and to attribute any differences to changes in horn allometry slope and/or intercept. Post-hoc pairwise intercept and slope comparisons were performed using estimated marginal means and Tukey contrasts (functions emmeans or emtrends in R package “emmeans”).<sup>152</sup>

Next, we compared *T. dichotomus* populations within the northern and southern clades separately. However, in contrast to *X. davidis*, horn-length body size scaling relationships in *T. dichotomus* are not linear, even when log-transformed,<sup>55,57,131,183–185</sup> so we also compared *T. dichotomus* populations by fitting the sigmoid equation:

$$\text{Horn length} \sim y_0 + \left( \left( a * (\text{Thorax width})^b \right) / \left( \left( (\text{Thorax width})^b \right) + c^b \right) \right) \quad (\text{Equation 2})$$

Where  $y_0$  is the minimum horn length,  $a$  is the horn length range,  $b$  is the curve steepness, and  $c$  is the body size (thorax width) at the inflection.<sup>186,187</sup> For both the northern and southern clade, we went through a model selection procedure to identify which parameters were better considered to be population-specific. We started by fitting the full model with all four parameters defined as population-specific and compared with four nested models each fixing one of the parameters as shared across populations. The model with the lowest Bayesian information criterion (BIC) was selected, and the procedure was repeated until no simpler model was found.

In contrast with the Akaike information criterion (AIC), BIC considers the sample size in addition to the goodness of fit and the number of parameters, and thus penalizes more complicated models when the sample size is large. It is therefore more conservative than AIC and considered more appropriate for large sample sizes (as is the case for most of the *Trypoxylus* populations<sup>188–190</sup>). Using the best selected model, we tested for pairwise population differences for the parameters fitted as population specific using the Bonferroni (conservative) and false discovery rate (less stringent) methods<sup>154,191</sup> to account for multiple testing arising from pairwise comparisons (function pairComp in package "aomisc"<sup>192</sup>). This permitted us to focus specific contrasts around the changes in horn length inferred from the phylogeny (i.e., not simply compare all populations to each other but compare before and after populations that bracket each inferred transition), and to describe more precisely how horn allometries evolved.

### Evolution of the horn lever system: head height, thoracic muscle area, and estimates of horn lifting force

Morphological variables were recorded from beetle specimens collected in the field and frozen or dried prior to transport. Measurements were made using digital calipers to the nearest 0.01 mm. Output lever of the horn system was the distance from the fulcrum hinge point at the back of the head to the end of the longest tine of the horn. Input lever of the horn system was the distance from the fulcrum to the insertion of the dorsal prothoracic muscle at the dorsal/caudal peak of the head. Prothorax width was measured at the widest point of the prothorax. Because we were dealing with frozen or dried specimens, muscle cross sectional area was estimated from the area of the sclerotized plate where the dorsal prothoracic muscle originates at the caudal end of the prothorax. Beetles were dissected, digital images were recorded of this plate, and area was calculated with ImageJ.<sup>193</sup>

Muscle force per cross sectional area in this species was estimated in a previous study by measuring lifting forces from live beetles, sacrificing them, then measuring lever and muscle morphology to calculate a force/cross sectional area.<sup>50</sup> This estimate was then used as a constant across all of the populations in this study to calculate horn lifting forces. Therefore, variation in our predictions of horn lifting forces (reported here) reflect changes in mechanical advantage and muscle cross sectional area across individuals and populations and does not include possible differences in muscle physiology.

Horn lifting forces were predicted using [Equation 1](#) with the following measures:

$$\text{Horn Lifting Force} = ((\text{Muscle Cross Sectional Area} * \text{Force} / \text{Cross Sectional Area}) * \text{Head Height}) / (\text{Horn Length}) \quad (\text{Equation 3})$$

Head height (input lever length), muscle cross-sectional area (input force), and horn lifting forces were first compared between the outgroup *X. davidis* and the two major *T. dichotomus* clades (i.e., northern and southern). For each biomechanical variable, we fitted a linear mixed model including  $\log_{10}$ -transformed head height, muscle cross-sectional area, or horn lifting forces as the response variable and  $\log_{10}$  thorax width, population, and their interaction as fixed effects (function lme, R package "nlme"). The population of origin was included as a random effect. Significance of the fixed effects was assessed using a type I (sequential) ANCOVA. Non-significant interactions ( $p > 0.1$ ) were removed from final analyses.<sup>194</sup> Post-hoc pairwise intercept and slope comparisons were performed using estimated marginal means and Tukey contrasts (functions emmeans or emtrends in R package "emmeans").<sup>152</sup>

We then compared *T. dichotomus* populations within the northern and southern clades separately.  $\log_{10}$ -transformed head height, muscle cross-sectional area, or horn lifting force was included as a response variable in a linear model, with  $\log_{10}$ -transformed prothorax width and population, and their interaction (if significant, i.e.,  $p < 0.1$ ) included as explanatory variables. Post-hoc pairwise comparisons between populations (intercept and slope if the interaction was significant) were performed using estimated marginal means and Tukey contrasts (functions emmeans or emtrends in R package "emmeans").

## Supplemental Information

### Evolution of horn length and lifting strength in the Japanese rhinoceros beetle

#### *Trypoxylus dichotomus*

Jesse N. Weber, Wataru Kojima, Romain P. Boisseau, Teruyuki Niimi, Shinichi Morita, Shuji Shigenobu, Hiroki Gotoh, Kunio Araya, Chung-Ping Lin, Camille Thomas-Bulle, Cerisse E. Allen, Wenfei Tong, Laura Corley Lavine, Brook O. Swanson, and Douglas J. Emlen

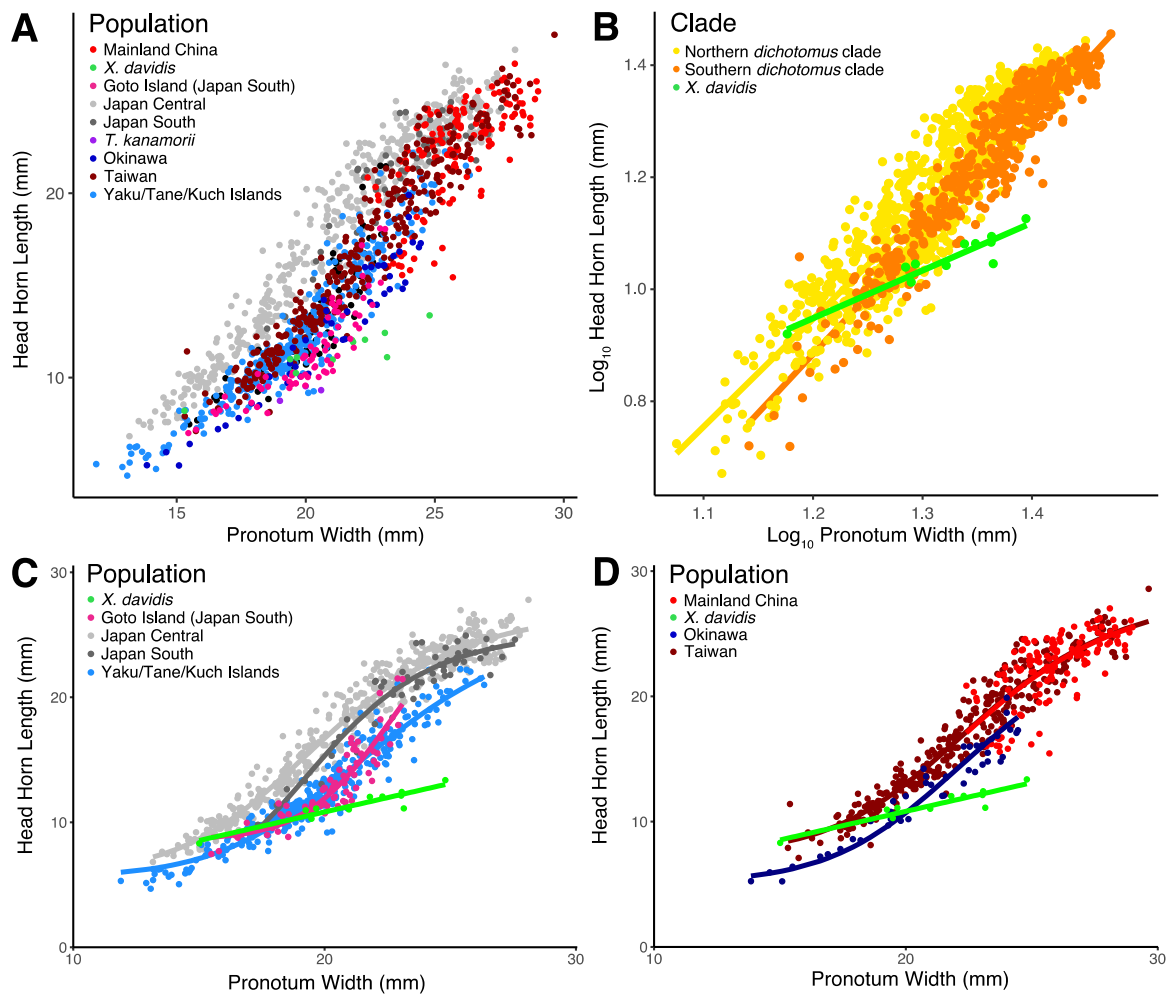
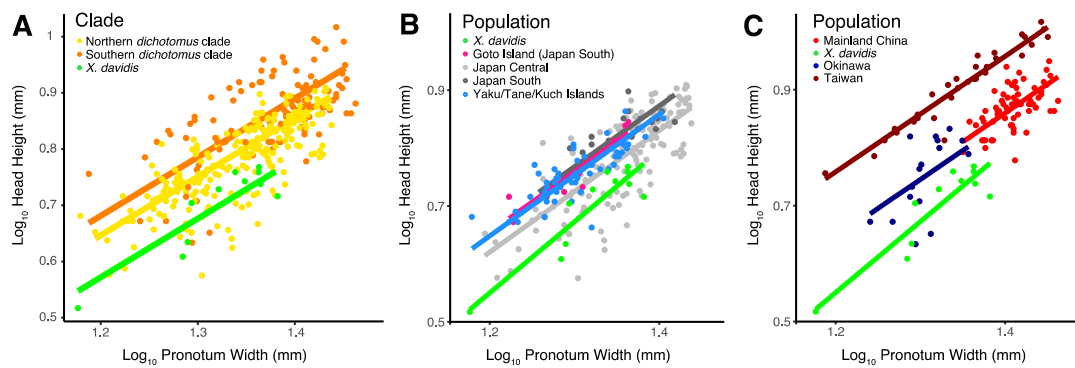
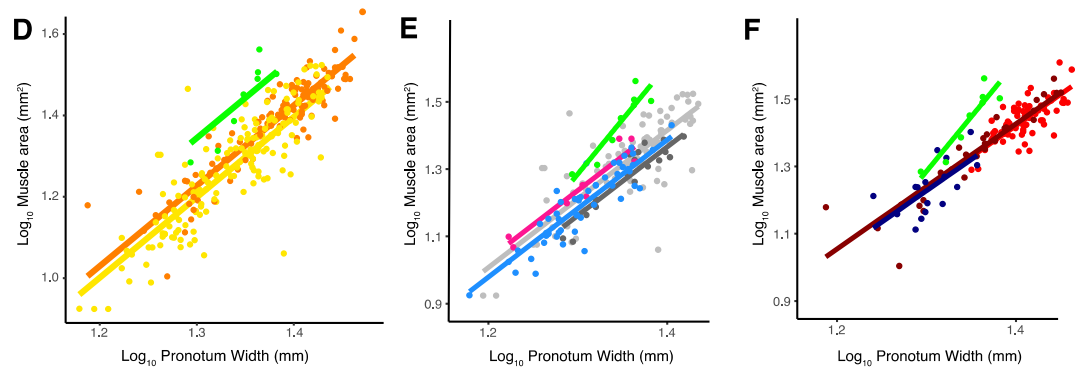


**Figure S1. Relationship between head horn length and pronotum width across all populations (A), main clades (B), northern clade populations (C), and southern clade populations (D). Related to Figures 3 and 4.** **A)** Horn length data for all populations **B)** Populations grouped into northern, southern, and *X. davidis*, for comparisons of scaling relationship slopes. See Table S1 for results of these analyses. **C)** Curve fits for comparisons of the scaling relationships between northern *Trypoxylus* populations. Results presented in Table S2. **D)** Curve fits for comparisons of the scaling relationships between southern *Trypoxylus* populations. Results presented in Table S3.

### Input lever length (head height)



### Muscle area



### Horn lifting force

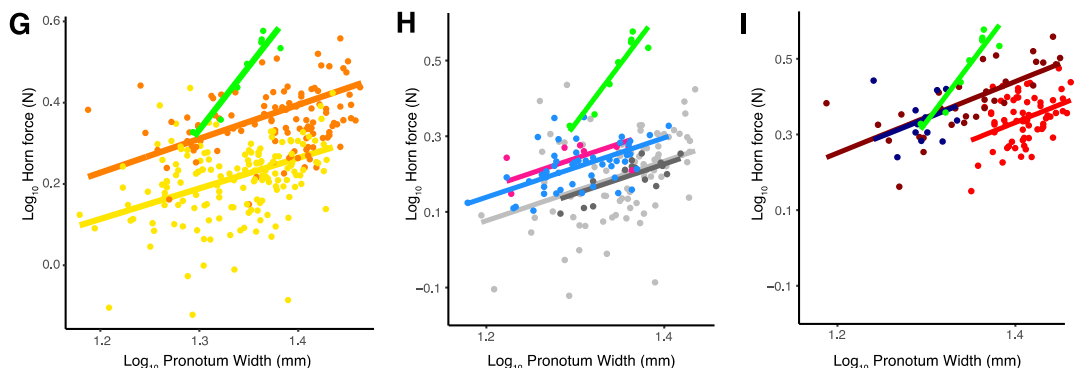


**Figure S2. Biomechanical variables (input lever length, muscle area, and estimated horn lifting force) as a function of pronotum width for all populations (A, D, G) and for the northern (B,E,H) and southern (C,F,I) clades separately. Related to Figures 3 and 4.**

Populations grouped into northern, southern, and *X. davidis*, for comparisons of **A**) input lever length (head height), **D**) thoracic (lifting) muscle size and **G**) horn lifting force. See Table S4 for results of these analyses. Comparisons of **B**) input lever length (head height), **E**) thoracic (lifting)

muscle size and **H**) horn lifting force for the Northern *Trypoxylylus* populations. See Table S5 for results of these analyses. Comparisons of **C**) input lever length (head height), **F**) thoracic (lifting) muscle size and **I**) horn lifting force for the Sourthern *Trypoxylylus* populations. See Table S6 for results of these analyses.

Response	Explanatory variables	F <sub>df1, df2</sub>	P value	Post-hoc tests
Log <sub>10</sub> (Horn length)	<b>Log<sub>10</sub> (Thorax width)</b>	<b>F<sub>1,1440</sub>= 15444</b>	<b>&lt;0.0001</b>	
	Population	F <sub>2,1440</sub> = 3.1	0.13	<u>Emmeans (intercept comparisons):</u> Davidis – North Clade: -0.14 ± 0.05, p=0.09 Davidis – South Clade: -0.10 ± 0.05, p=0.24 North Clade – South Clade: -0.04 ± 0.035, p=0.52
	<b>Interaction</b>	<b>F<sub>2,1440</sub>= 25.4</b>	<b>&lt;0.0001</b>	<u>Emtrends (slope comparisons):</u> Davidis – North Clade: -1.07 ± 0.20, p<0.0001 Davidis – South Clade: -1.24 ± 0.20, p<0.0001 North Clade – South Clade: -0.17 ± 0.04, p<0.0001

**Table S1. Analyses of the differences between the outgroup (*X. davidis*) and northern and southern lineages of *T. dichotomus*, in the scaling relationship between male horn length and body size (thorax width). Related to Figures 3 and 4.** A linear mixed model including population of origin as a random intercept was fit and the results of a type I ANCOVA are presented here. Post hoc pairwise comparisons using estimated marginal means and Tukey contrasts (functions emmeans or emtrends in R package “emmeans”) are reported for categorical variables. Significant effects are bolded (P < 0.05).

Model parameter	Japan Central	Japan South	Goto	Yakushima	F	P	$\Delta$ AIC (Full model AIC = 2950)	$\Delta$ BIC (Full model BIC = 3033)
<b>y0</b>	<b>6.62±0.48</b>	<b>7.82 ±2.5</b>	<b>8.53±0.73</b>	<b>5.31 ±0.52</b>	<b>6.95</b>	<b>0.0001</b>	-14.96	-0.39
a	20.22±0.85	16.74±3.11	23.91±19.75	23.91±3.52	2.37	0.07	-1.21	13.34
<b>b</b>	<b>7.40±0.47</b>	<b>11.32±2.80</b>	<b>11.40±4.42</b>	<b>6.00±0.75</b>	<b>8.38</b>	<b>&lt;0.0001</b>	-19.22	-4.65
<b>c</b>	<b>20.01±0.13</b>	<b>20.50±0.56</b>	<b>23.42±2.92</b>	<b>22.94±0.91</b>	<b>32.6</b>	<b>&lt;0.0001</b>	-88.58	-74.01

Parameter	Pair	Contrast ± SE	P (Bonferroni)	P (FDR)
y0 (Minimum horn length)	<b>Japan Central – Japan South</b>	<b>1.88 ± 0.75</b>	0.07	<b>0.018</b>
	<b>Japan Central – Goto</b>	<b>-2.52 ± 0.67</b>	<b>0.001</b>	<b>0.0004</b>
	Japan Central – Yakushima	0.41 ± 0.49	1	0.40
	<b>Japan South – Goto</b>	<b>-4.40 ± 1.09</b>	<b>0.0003</b>	<b>0.0002</b>
	Japan South – Yakushima	-1.46 ± 0.96	0.76	0.15
	<b>Goto – Yakushima</b>	<b>2.93 ± 0.54</b>	<b>&lt;0.0001</b>	<b>&lt;0.0001</b>
b (Steepness)	<b>Japan Central – Japan South</b>	<b>-1.68 ± 0.75</b>	0.15	<b>0.03</b>
	<b>Japan Central – Goto</b>	<b>-5.15 ± 1.20</b>	<b>0.0001</b>	<b>&lt;0.0001</b>
	Japan Central – Yakushima	0.25 ± 0.27	1	0.37
	<b>Japan South – Goto</b>	<b>-3.47 ± 1.40</b>	0.08	<b>0.02</b>
	<b>Japan South – Yakushima</b>	<b>1.93 ± 0.77</b>	0.08	<b>0.02</b>
	<b>Goto – Yakushima</b>	<b>5.40 ± 1.21</b>	<b>&lt;0.0001</b>	<b>&lt;0.0001</b>
c (Thorax width at inflection point)	Japan Central – Japan South	0.21 ± 0.38	1	0.59
	<b>Japan Central – Goto</b>	<b>-3.02 ± 0.27</b>	<b>&lt;0.0001</b>	<b>&lt;0.0001</b>
	<b>Japan Central – Yakushima</b>	<b>-2.31 ± 0.34</b>	<b>&lt;0.0001</b>	<b>&lt;0.0001</b>
	<b>Japan South – Goto</b>	<b>-3.23 ± 0.47</b>	<b>&lt;0.0001</b>	<b>&lt;0.0001</b>
	<b>Japan South – Yakushima</b>	<b>-2.51 ± 0.53</b>	<b>&lt;0.0001</b>	<b>&lt;0.0001</b>
	<b>Goto – Yakushima</b>	<b>0.72 ± 0.26</b>	<b>0.04</b>	<b>0.008</b>

**Table S2. Allometric differences between populations of the northern clade. Related to**

**Figure 3. Top:** A non-linear least square regression was fit to the horn length / body size distributions of the four northern populations. Curve parameters were considered different between populations. To test for significant differences between populations for each parameter, we compared the full model with a model assuming that all populations had the same given parameter, using an ANOVA, and differences in AIC and BIC (full – reduced model). **Bottom:** Post-hoc pairwise differences in allometric parameters between northern populations. All curve parameters were considered different between populations, except "a" (horn length range) as this was the best model based on BIC. P-values were adjusted using the Bonferroni or False Discovery Rate method to account for multiple pairwise testing. Significant effects are bolded (P < 0.05).

Model parameter	Taiwan	Mainland China	Okinawa	F	P	$\Delta$ AIC (Full model AIC = 1782)	$\Delta$ BIC (Full model BIC = 1837)
<b>y0</b>	<b>7.71±0.76</b>	<b>10.9 ±18.5</b>	<b>3.74±3.31</b>	<b>2.98</b>	<b>0.05</b>	-2.08	6.30
a	20.45±1.85	16.74±23.04	23.91±23.35	0.31	0.74	3.37	11.75
b	8.12±0.99	9.03±11.15	5.40±4.39	0.54	0.59	2.90	11.28
c	22.8 ±0.28	23.62±4.45	23.08±6.38	0.26	0.77	3.47	11.85

Parameter	Pair	Contrast ± SE	P (Bonferroni)	P (FDR)
y0 (Minimum horn length)	Taiwan – Mainland China	0.08 ± 0.18	1	0.67
	Taiwan – Okinawa	<b>2.29 ± 0.24</b>	<0.0001	<0.0001
	China – Okinawa	<b>2.21 ± 0.29</b>	<0.0001	<0.0001

**Table S3. Allometric differences between populations of the southern clade. Related to**

**Figure 4. Top:** A non-linear least square regression was fit to the horn length / body size distributions of the three southern populations. Curve parameters were considered different between populations. To test for significant differences between populations for each parameter, we compared the full model with a model assuming that all populations had the same given parameter, using an ANOVA, and differences in AIC and BIC (full – reduced model). **Bottom:** Post-hoc pairwise differences in allometric parameters between southern populations. All curve parameters were considered identical between populations, except "y0" (minimum horn length) as this was the best model based on BIC. P-values were adjusted using the Bonferroni or False Discovery Rate method to account for multiple pairwise testing. Significant effects are bolded (P < 0.05).

Response	Explanatory variables	F <sub>df1, df2</sub>	P value	Post-hoc tests
<b>Input lever length</b>				
Log <sub>10</sub> (Input lever length)	<b>Log<sub>10</sub> (Thorax width)</b>	<b>F<sub>1,343</sub>= 583.7</b>	<b>&lt;0.0001</b>	-
	Lineage	F <sub>2,5</sub> = 3.89	0.10	-
	Interaction	F <sub>2,343</sub> = 0.48	0.62	-
Log <sub>10</sub> (Input lever length)	<b>Log<sub>10</sub> (Thorax width)</b>	<b>F<sub>1,345</sub>= 585.5</b>	<b>&lt;0.0001</b>	-
	Lineage	F <sub>2,5</sub> = 3.90	0.095	Emmeans (intercept comparisons): Davidis – North Clade: -0.07 ± 0.04, p=0.22 Davidis – South Clade: -0.11 ± 0.04, p=0.085 North – South Clade: -0.03 ± 0.03, p=0.42
<b>Muscle area</b>				
Log <sub>10</sub> (Muscle area)	<b>Log<sub>10</sub> (Thorax width)</b>	<b>F<sub>1,268</sub>= 819.2</b>	<b>&lt;0.0001</b>	-
	Lineage	F <sub>2,5</sub> = 17.79	<b>0.005</b>	-
	Interaction	F <sub>2,268</sub> = 1.80	0.17	-
Log <sub>10</sub> (Muscle area)	<b>Log<sub>10</sub> (Thorax width)</b>	<b>F<sub>1,270</sub>= 803.8</b>	<b>&lt;0.0001</b>	-
	Lineage	F <sub>2,5</sub> = 17.18	<b>0.006</b>	Emmeans (intercept comparisons): <b>Davidis – North Clade: 0.15 ± 0.026, p=0.005</b> <b>Davidis – South Clade: 0.12 ± 0.026, p=0.014</b> North – South Clade: -0.03 ± 0.012, p=0.13
<b>Lifting force</b>				
Log <sub>10</sub> (Lifting force)	<b>Log<sub>10</sub> (Thorax width)</b>	<b>F<sub>1,265</sub>= 73.98</b>	<b>&lt;0.0001</b>	-
	Lineage	F <sub>2,5</sub> = 16.74	<b>0.006</b>	Emmeans (intercept comparisons): <b>Davidis – North Clade: 0.28 ± 0.051, p=0.007</b> Davidis – South Clade: 0.15 ± 0.05, p=0.075 <b>North – South Clade: -0.13 ± 0.031, p=0.021</b>
	Interaction	F <sub>2,265</sub> = 2.78	0.064	Emtrends (slope comparisons): <b>Davidis – North Clade: 2.37 ± 1.01, p=0.05</b> Davidis – South Clade: 2.29 ± 1.02, p=0.065 North – South Clade: -0.084 ± 0.21, p=0.91

**Table S4: Analyses of the differences between the outgroup (*X. davidis*) and northern and southern lineages of *T. dichotomus* in the scaling relationship between male body size (thorax width) and input lever length (head height), thoracic (lifting) muscle size, and horn lifting force. Related to Figures 3 and 4.** Two linear mixed models including population of origin as a random intercept were fit, including the interaction between predictors or not, and the results of type I ANCOVAs are presented here. Post hoc pairwise intercept comparisons using estimated marginal means and Tukey contrasts (function emmeans in R package “emmeans”) are reported. Significant effects are bolded (P < 0.05).

Response	Explanatory variables	F <sub>df1, df2</sub>	P value	Post-hoc tests
<b>Input lever length</b>				
Log <sub>10</sub> (Input lever length)	<b>Log<sub>10</sub> (Thorax width)</b>	<b>F<sub>1,221</sub> = 376.0</b>	<b>&lt;0.0001</b>	-
	<b>Northern population</b>	<b>F<sub>3,221</sub> = 9.47</b>	<b>&lt;0.0001</b>	-
	Interaction	F <sub>3,221</sub> = 1.82	0.14	-
Log <sub>10</sub> (Input lever length)	<b>Log<sub>10</sub> (Thorax width)</b>	<b>F<sub>1,224</sub> = 372.0</b>	<b>&lt;0.0001</b>	-
	<b>Northern population</b>	<b>F<sub>3,224</sub> = 9.37</b>	<b>&lt;0.0001</b>	Emmeans (intercept comparisons): Goto – Japan Central: 0.03 ± 0.016, p=0.145 Goto – Japan South: -0.009 ± 0.018, p=0.96 Goto – Yakushima: 0.006 ± 0.016, p=0.98 <b>Japan Central – Japan South: -0.04 ± 0.01, p=0.003</b> <b>Japan Central – Yakushima: -0.028 ± 0.008, p=0.001</b> Japan South – Yakushima: 0.015 ± 0.012, p=0.58
<b>Muscle area</b>				
Log <sub>10</sub> (Muscle area)	<b>Log<sub>10</sub> (Thorax width)</b>	<b>F<sub>1,151</sub> = 465.6</b>	<b>&lt;0.0001</b>	-
	<b>Northern population</b>	<b>F<sub>3,151</sub> = 4.42</b>	<b>0.005</b>	-
	Interaction	F <sub>3,151</sub> = 0.50	0.68	-
Log <sub>10</sub> (Muscle area)	<b>Log<sub>10</sub> (Thorax width)</b>	<b>F<sub>1,154</sub> = 470.3</b>	<b>&lt;0.0001</b>	-
	<b>Northern population</b>	<b>F<sub>3,154</sub> = 4.47</b>	<b>0.005</b>	Emmeans (intercept comparisons): Goto – Japan Central: 0.025 ± 0.025, p=0.76 Goto – Japan South: 0.074 ± 0.029, p=0.057 Goto – Yakushima: 0.053 ± 0.025, p=0.15 <b>Japan Central – Japan South: 0.049 ± 0.018, p=0.03</b> Japan Central – Yakushima: 0.028 ± 0.013, p=0.13 Japan South – Yakushima: -0.021 ± 0.019, p=0.71
<b>Lifting force</b>				
Log <sub>10</sub> (Lifting force)	<b>Log<sub>10</sub> (Thorax width)</b>	<b>F<sub>1,150</sub> = 18.32</b>	<b>&lt;0.0001</b>	-
	<b>Northern population</b>	<b>F<sub>3,150</sub> = 6.22</b>	<b>0.0005</b>	-
	Interaction	F <sub>3,150</sub> = 0.45	0.72	-
Log <sub>10</sub> (Lifting force)	<b>Log<sub>10</sub> (Thorax width)</b>	<b>F<sub>1,153</sub> = 18.53</b>	<b>&lt;0.0001</b>	-
	<b>Northern population</b>	<b>F<sub>3,153</sub> = 6.29</b>	<b>0.0005</b>	Emmeans (intercept comparisons): <b>Goto – Japan Central: 0.09 ± 0.03, p=0.04</b> Goto – Japan South: 0.09 ± 0.04, p=0.066 Goto – Yakushima: 0.024 ± 0.032, p=0.87 Japan Central – Japan South: 0.008 ± 0.023, p=0.99 <b>Japan Central – Yakushima: -0.06 ± 0.02, p=0.001</b> <b>Japan South – Yakushima: -0.069 ± 0.025, p=0.037</b>

**Table S5: Analyses of the differences between northern *Trypoxylus* populations in the scaling relationship between male body size (thorax width) and input lever length (head height), thoracic (lifting) muscle size, and horn lifting force. Related to Figure 3.**

Two linear models were fit, including the interaction between predictors or not, and the results of type I ANCOVAs are presented here. Post hoc pairwise intercept comparisons using estimated marginal means and Tukey contrasts (function emmeans in R package “emmeans”) are reported between northern populations. Significant effects are bolded (P < 0.05).

Response	Explanatory variables	F <sub>df1, df2</sub>	P value	Post-hoc tests
<b>Input lever length</b>				
Log <sub>10</sub> (Input lever length)	<b>Log<sub>10</sub> (Thorax width)</b>	<b>F<sub>1,108</sub> = 219.0</b>	<b>&lt;0.0001</b>	-
	<b>Southern population</b>	<b>F<sub>2,108</sub> = 103.3</b>	<b>&lt;0.0001</b>	-
	Interaction	F <sub>2,108</sub> = 1.96	0.15	-
Log <sub>10</sub> (Input lever length)	<b>Log<sub>10</sub> (Thorax width)</b>	<b>F<sub>1,110</sub> = 215.2</b>	<b>&lt;0.0001</b>	-
	<b>Southern population</b>	<b>F<sub>2,110</sub> = 101.6</b>	<b>&lt;0.0001</b>	Emmeans (intercept comparisons): Mainland China – Okinawa: 0.015 ± 0.012, p=0.44 Mainland China – Taiwan: -0.098 ± 0.009, p<0.0001 Okinawa – Taiwan: -0.113 ± 0.011, p<0.0001
<b>Muscle area</b>				
Log <sub>10</sub> (Muscle area)	<b>Log<sub>10</sub> (Thorax width)</b>	<b>F<sub>1,106</sub> = 529.3</b>	<b>&lt;0.0001</b>	-
	Southern population	F <sub>2,106</sub> = 0.36	0.70	-
	Interaction	F <sub>2,106</sub> = 0.90	0.41	-
Log <sub>10</sub> (Muscle area)	<b>Log<sub>10</sub> (Thorax width)</b>	<b>F<sub>1,108</sub> = 530.3</b>	<b>&lt;0.0001</b>	-
	Southern population	F <sub>2,108</sub> = 0.36	0.70	Emmeans (intercept comparisons): Mainland China – Okinawa: 0.008 ± 0.018, p=0.91 Mainland China – Taiwan: -0.005 ± 0.013, p=0.91 Okinawa – Taiwan: -0.013 ± 0.016, p=0.70
<b>Lifting force</b>				
Log <sub>10</sub> (Lifting force)	<b>Log<sub>10</sub> (Thorax width)</b>	<b>F<sub>1,104</sub> = 11.28</b>	<b>0.001</b>	-
	<b>Southern population</b>	<b>F<sub>2,104</sub> = 24.78</b>	<b>&lt;0.0001</b>	-
	Interaction	F <sub>2,104</sub> = 1.16	0.32	-
Log <sub>10</sub> (Lifting force)	<b>Log<sub>10</sub> (Thorax width)</b>	<b>F<sub>1,106</sub> = 11.25</b>	<b>0.001</b>	-
	<b>Southern population</b>	<b>F<sub>2,106</sub> = 24.71</b>	<b>&lt;0.0001</b>	Emmeans (intercept comparisons): Mainland China – Okinawa: -0.11 ± 0.024, p=0.0001 Mainland China – Taiwan: -0.01 ± 0.016, p<0.0001 Okinawa – Taiwan: -0.003 ± 0.021, p=0.99

**Table S6: Analyses of the differences between southern *Trypoxylus* populations in the scaling relationship between male body size (thorax width) and input lever length (head height), thoracic (lifting) muscle size, and horn lifting force. Related to Figure 4.** Two linear models were fit, including the interaction between predictors or not, and the results of type I ANCOVAs are presented here. Post hoc pairwise intercept comparisons using estimated marginal means and Tukey contrasts (function emmeans in R package “emmeans”) are reported between northern populations. Significant effects are bolded (P < 0.05).